

Chapter III

RESULTS

AND

DISCUSSION

RESULTS AND DISCUSSION

III.1. Chemical Structure Confirmation of Surfactants

Aqueous fire fighting foams (AFFF) are used to put out polar and nonpolar liquid materials fires such as petroleum oil, alcohols, ketones, and esters. They are prepared from specific aqueous formulations, named foam concentrates diluted with water and applied with a nozzle under the form of aqueous foam, which contain over 80% air. Their very low apparent density allows them to be deposited at the surface of burning liquids. The evaporation of the water resulting from the heat reduces the intensity of the fire and the foam generates a water film at the surface of the burning materials, which prevents the emission of flammable vapors. In addition, after extinction, the foam prevents the risk of fire burn back. As a result of foams advantages, twelve surfactants were prepared to test them as AFFF materials in area of petroleum industry. These surfactants based on dodecylbenzene sulfonic acid (9 surfactants) and dodecylphenol (3 surfactants). The preparation reactions were followed using the FT.ir as shown in *Figs. 8 to 16*, the preparation steps are shown in *Schemes 1 to 3*.

III.1.1. Preparation of AFFF Based on Dodecylbenzene Sulfonic Acid

The FT.ir of the prepared lauroylbenzene is shown in *Fig.8*, the characteristic bands are; a band at 1680 cm^{-1} indicating the presence of (C=O) group, a band at 1220 cm^{-1} assigned to

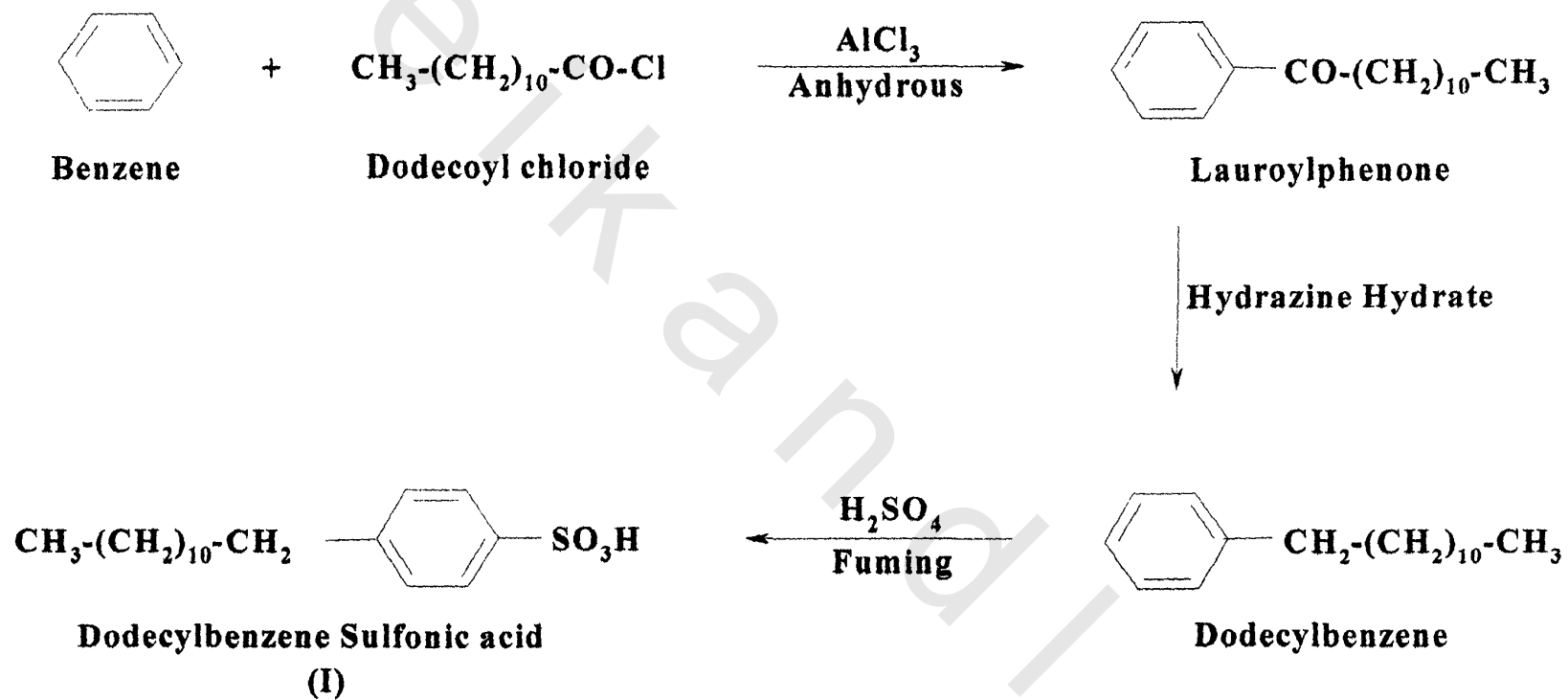
stretching and bending vibrations of the C-CO-C group, also a band at 3025 cm^{-1} assigned to C-H ring stretching vibration, bands at 2900 and 2830 cm^{-1} for asymmetric and symmetric C-H stretching of linear alkyl chain, a band at 1590 cm^{-1} pinoted to C=C ring stretching, bands at 1450 and 1360 cm^{-1} refered to C-H deformation of CH_2 - and CH_3 - groups respectively, and finally the bands at 760 and 700 cm^{-1} that pointing to C-H ring deformation which confirm the mono substitution ring.

The lauroylbenzene was reduced using Huan-Minlon reduction method to form linear dodecylbenzene. The FT.ir cleared in *Fig. 9*, where the disappearance of the band at 1680 cm^{-1} assigned to the C=O group and that at 1220 cm^{-1} pointed to the C-CO-C group. This confirms the completion of the reduction reaction.

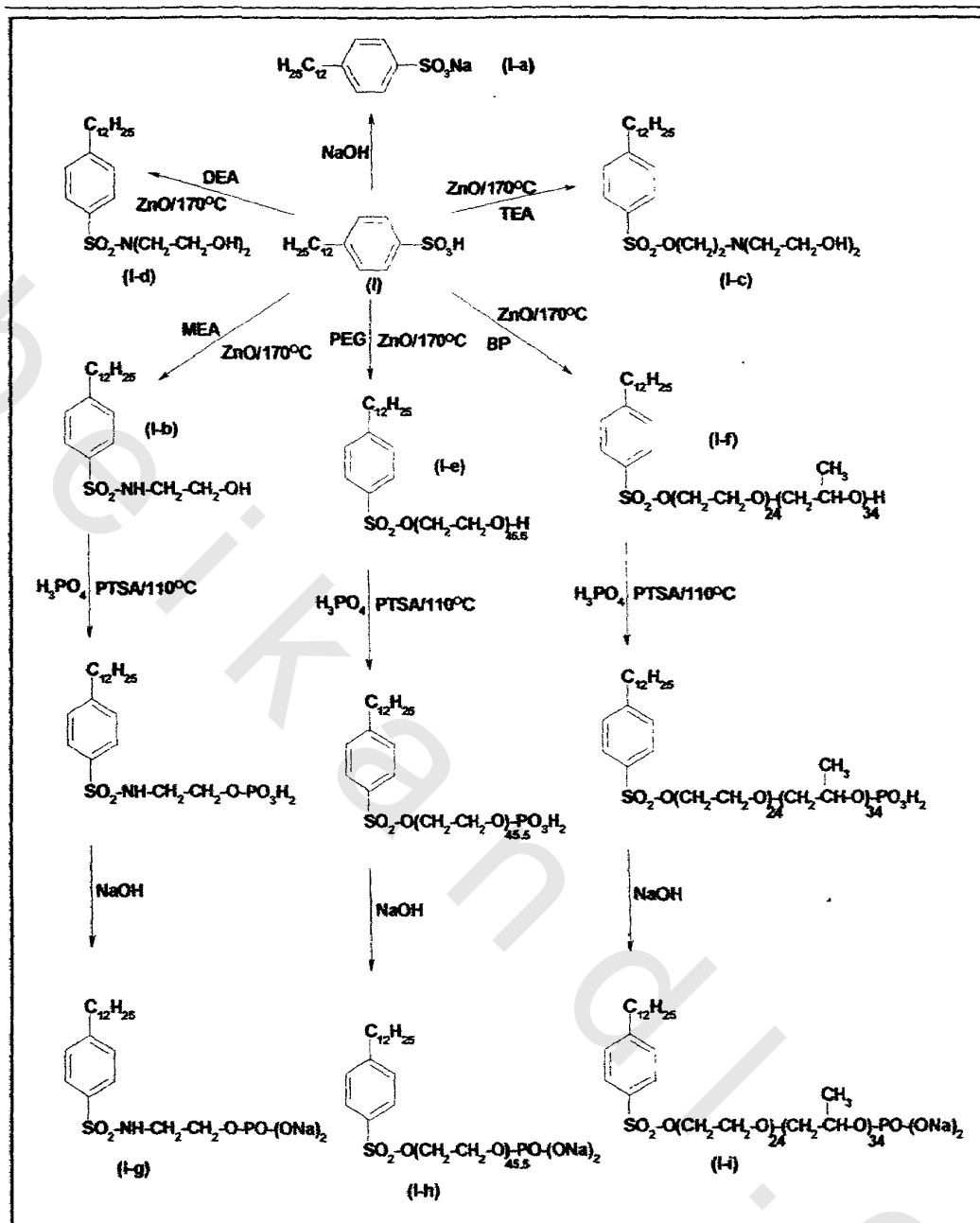
The confirmation of sulfonation reaction for dodecylbenzene was remarked by spectrum showed in *Fig. 10*, where a strong bands at 1192 and 1042 cm^{-1} characteristic for asymmetric and symmetric S=O group (stretching vibrations) respectively. A band at 684 cm^{-1} assigned to the S-O group. These four bands confirm the presence of sulfonic acid group ($-\text{SO}_3\text{H}$). Also, the appearance of a band at 830 cm^{-1} pointed to p-substitution of benzene ring with the disappearance of bands at 760 and 700 cm^{-1} confirms the presence of p-substituted ring rather than mono substitution.

Fig. 11, shows the FT.ir spectrum of 4-dodecylbenzene N-ethanol sulfonamide. In the spectrum, a more broad band for overlapped O-H and N-H groups appears in the range of 3310-3540 cm^{-1} . Also, there are two bands at 1338 and 1131 cm^{-1} characteristic for S-N group. These three bands indicates the presence of sulfonamide group and confirme the amidation reaction.

The spectra of the end product (4-dodecylbenzene N-ethanol phosphate sulfonamide), is shown in *Fig. 12*, where besidesat the characteristic bands of DBMSA(I-b) the chart shows two bands at 1042, 2371 cm^{-1} characteristic for P-OH group, and a band at 1009 cm^{-1} assigned to C-O-P group. All of these bands are referring to the presence of phosphate group and confirming that the phosphorylation reaction was completely occurred.



Scheme 1: preparation of dodecylbenzene sulfonic acid



Where; MEA is monoethanol amine.

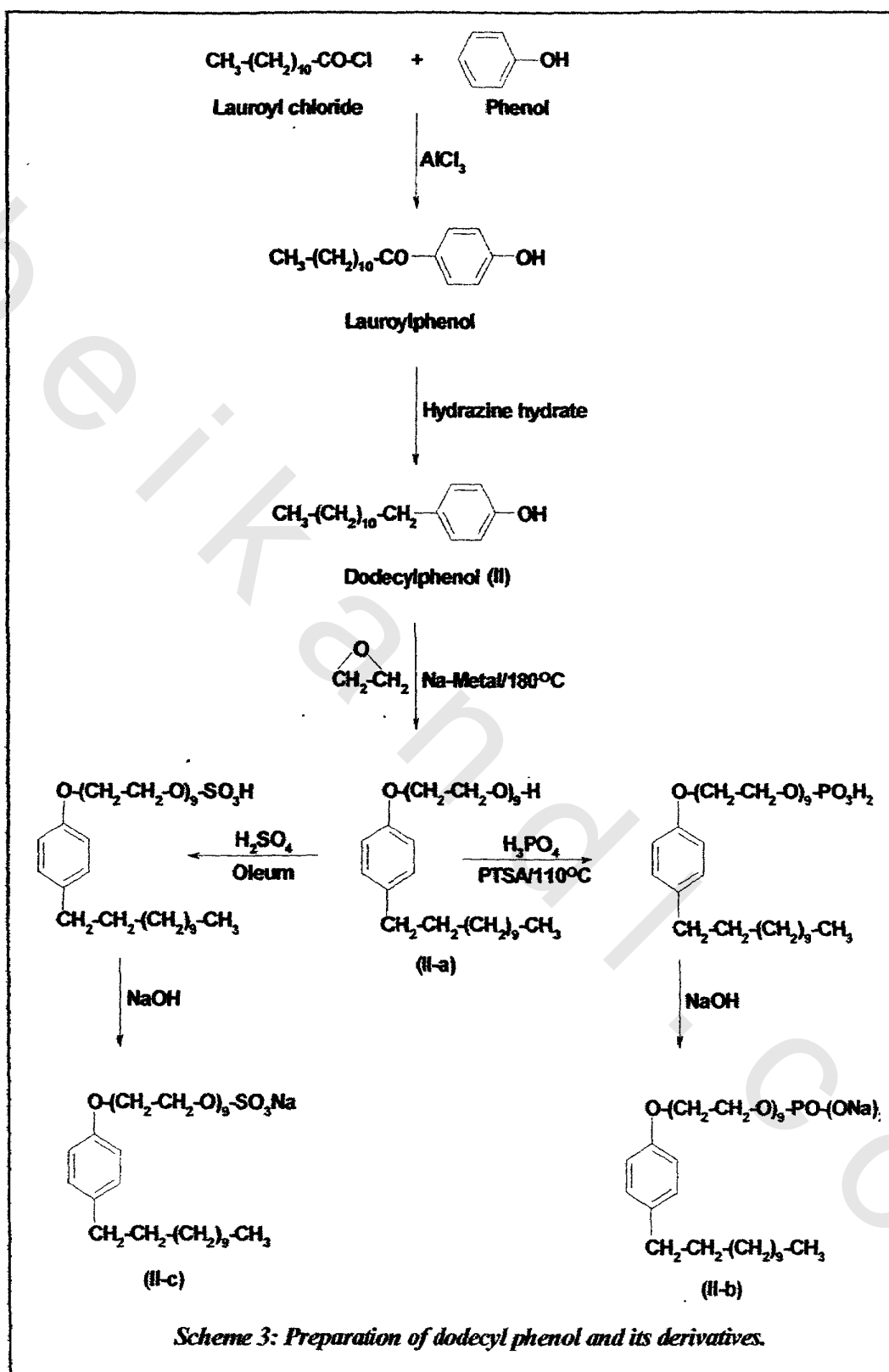
DEA is diethanol amine.

TEA is triethanol amine.

PEG is polyethylene glycol.

BP is ethylene oxide (e.o,24)-propylene oxide (p.o,34) block Co-polymer.

Scheme 2: Preparation of dodecylbenzene sulfonic acid derivatives



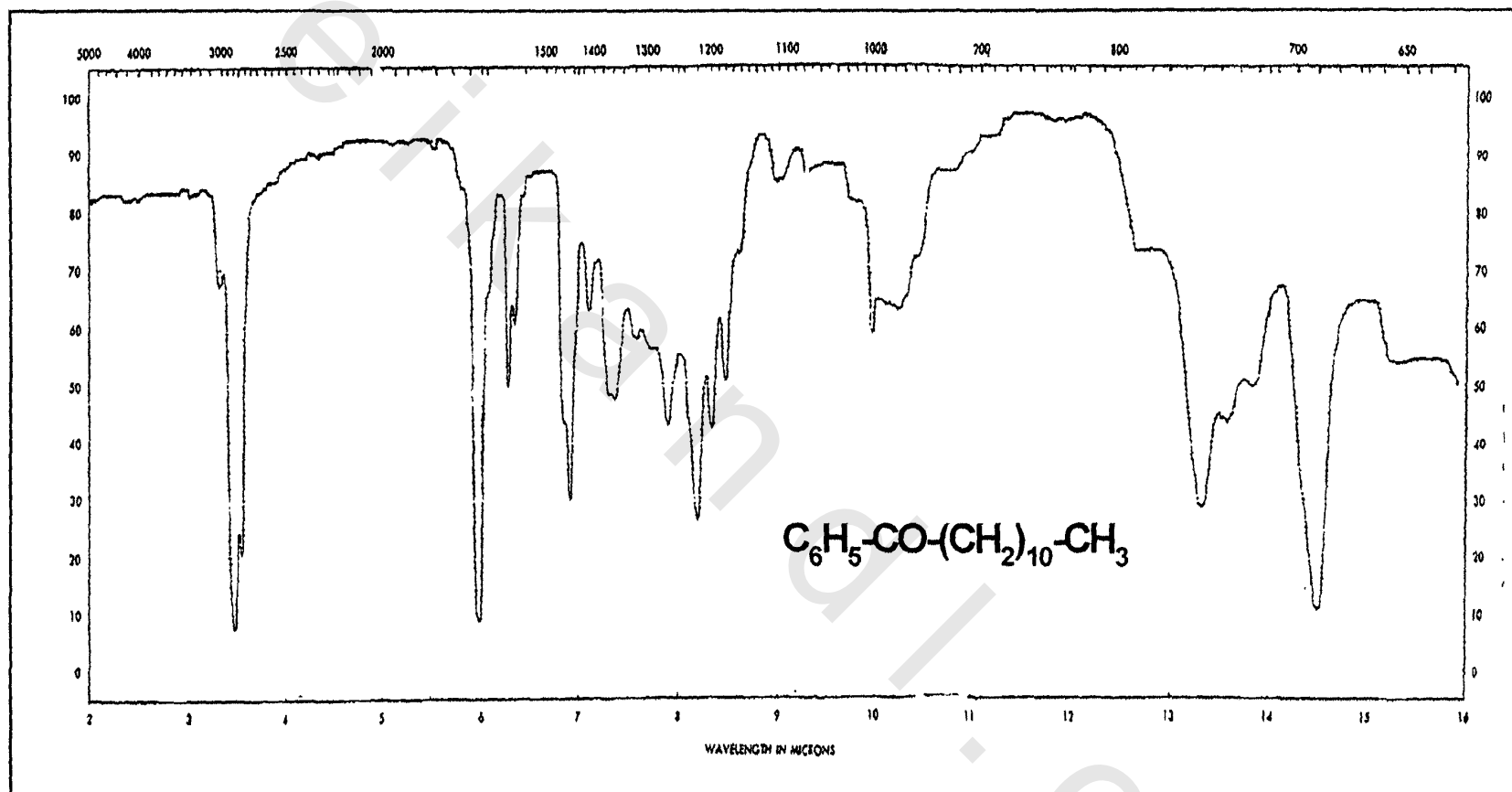


Fig. 8: FT.ir of Lauroylbenzene

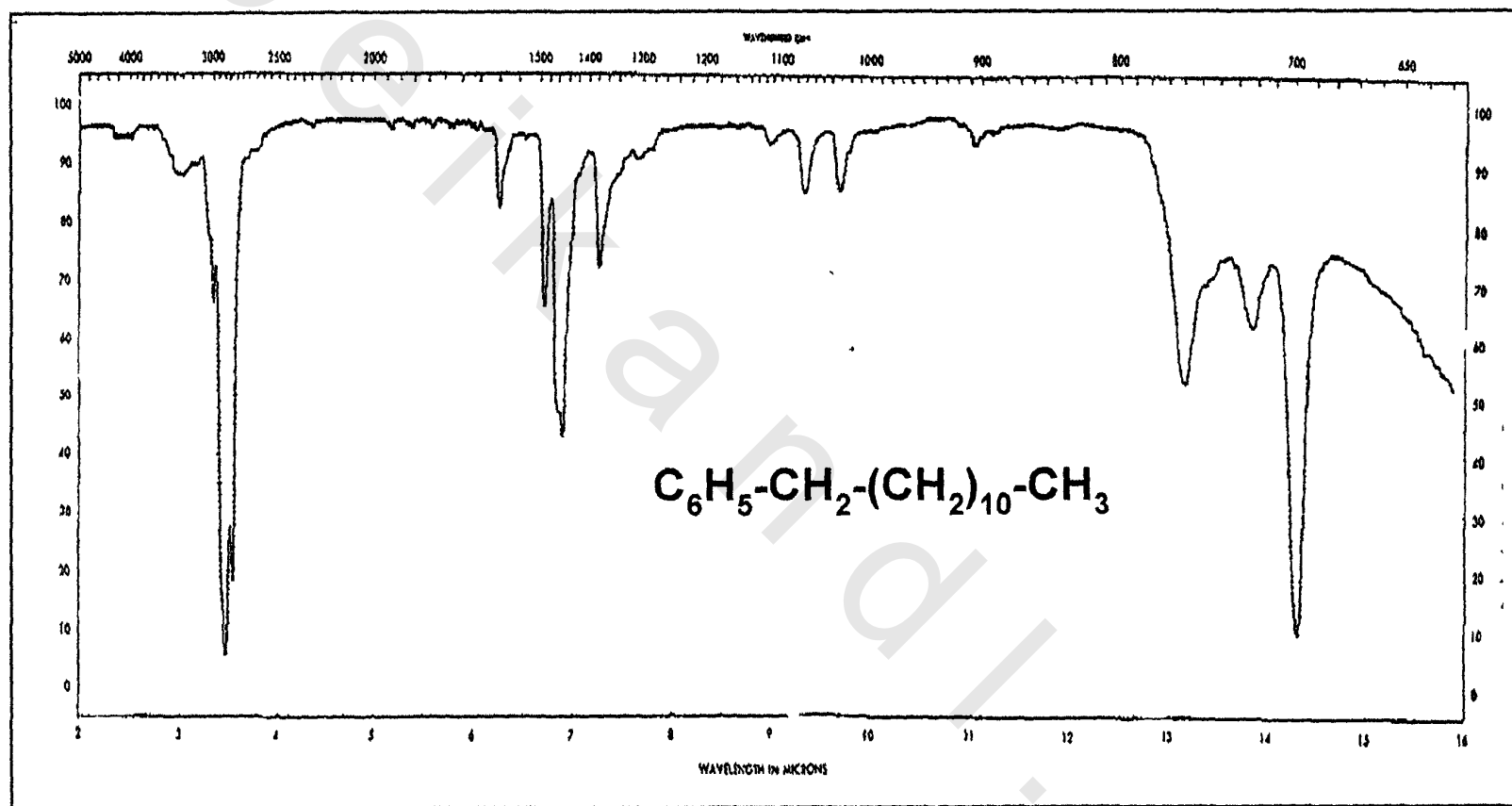


Fig. 9: FT.ir of Dodecylbenzene

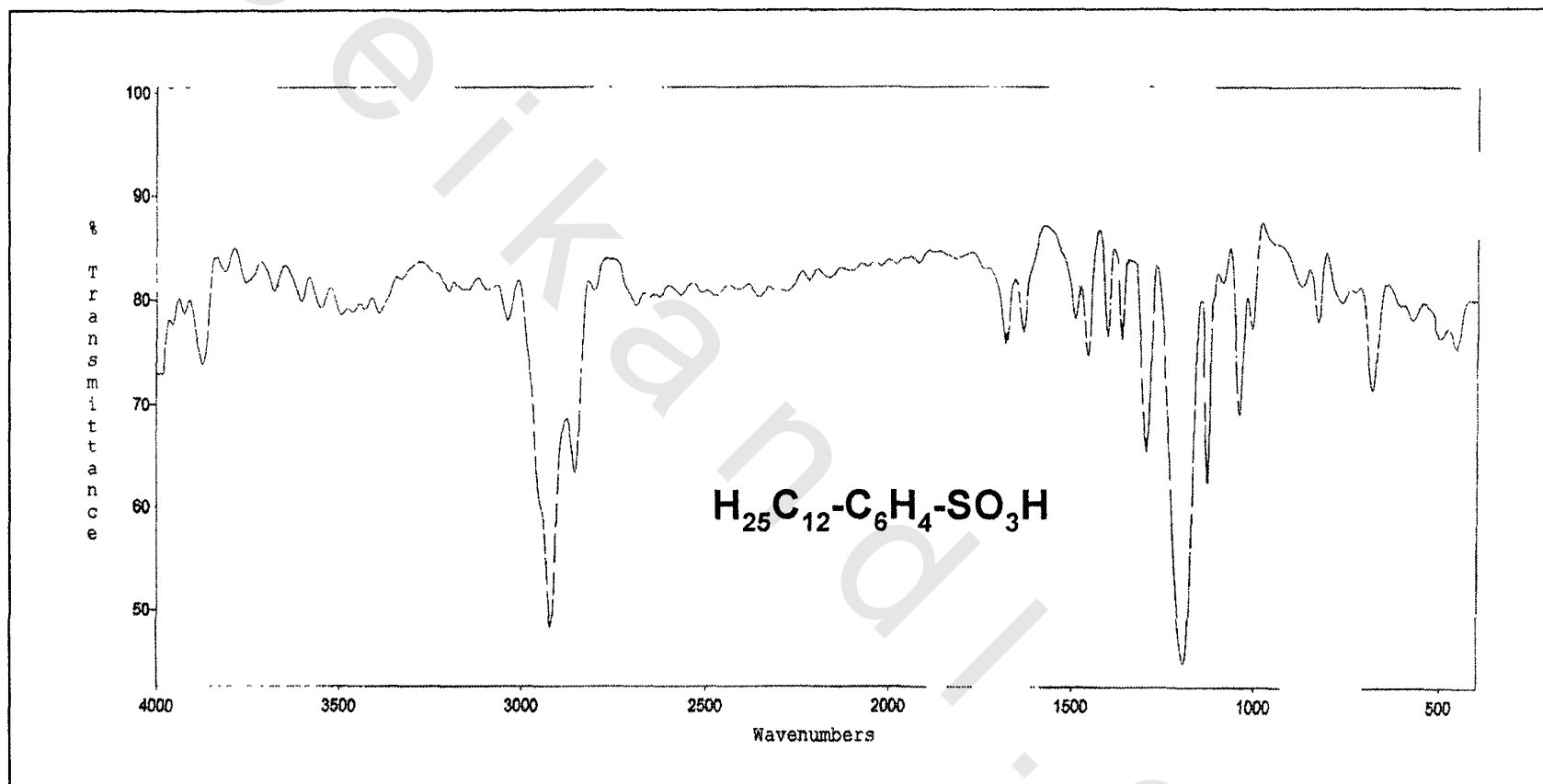


Fig. 10: FT.ir of Dodecylbenzene Sulfonic Acid

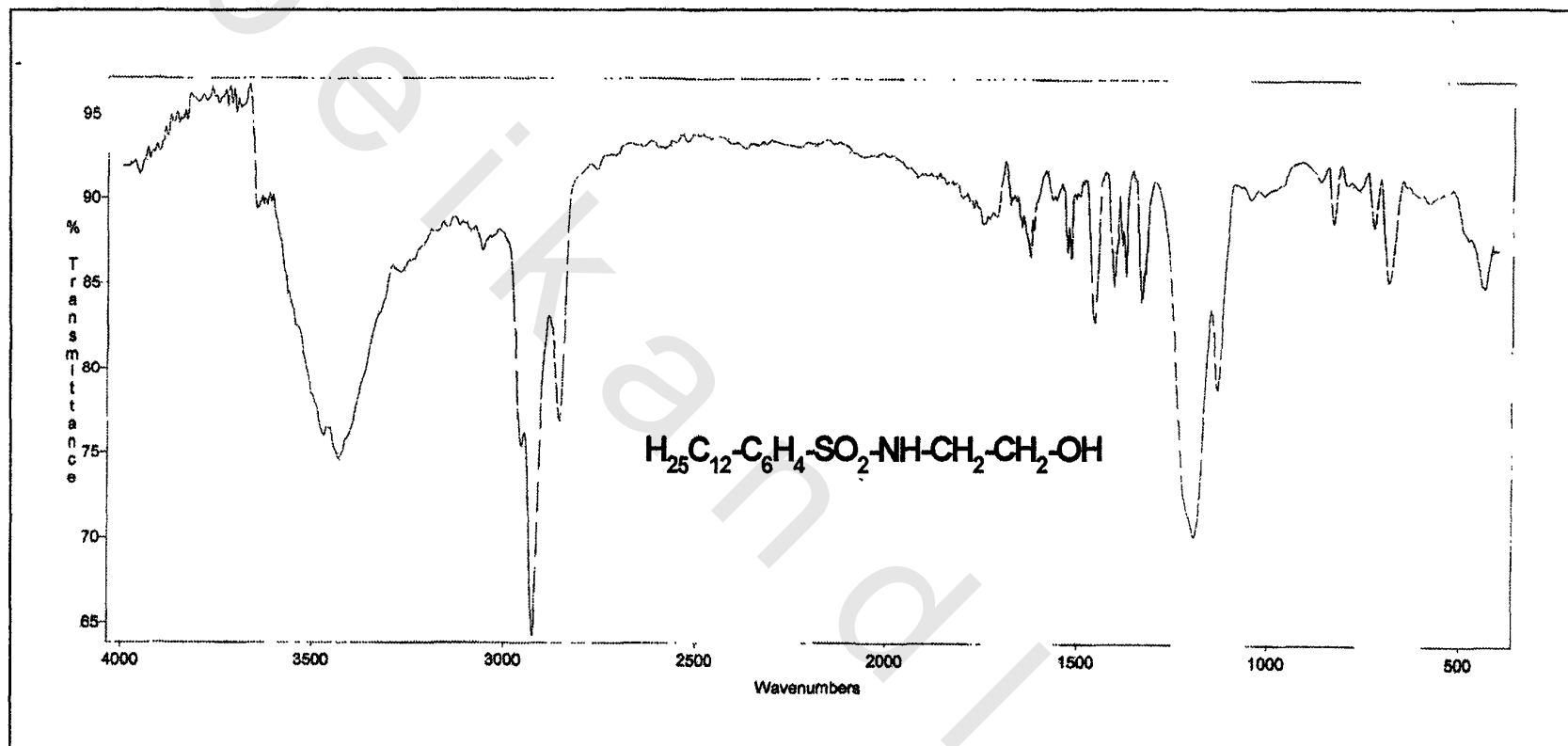


Fig. 11: FT.ir of 4-dodecyl N-ethanol sulfonamide benzene

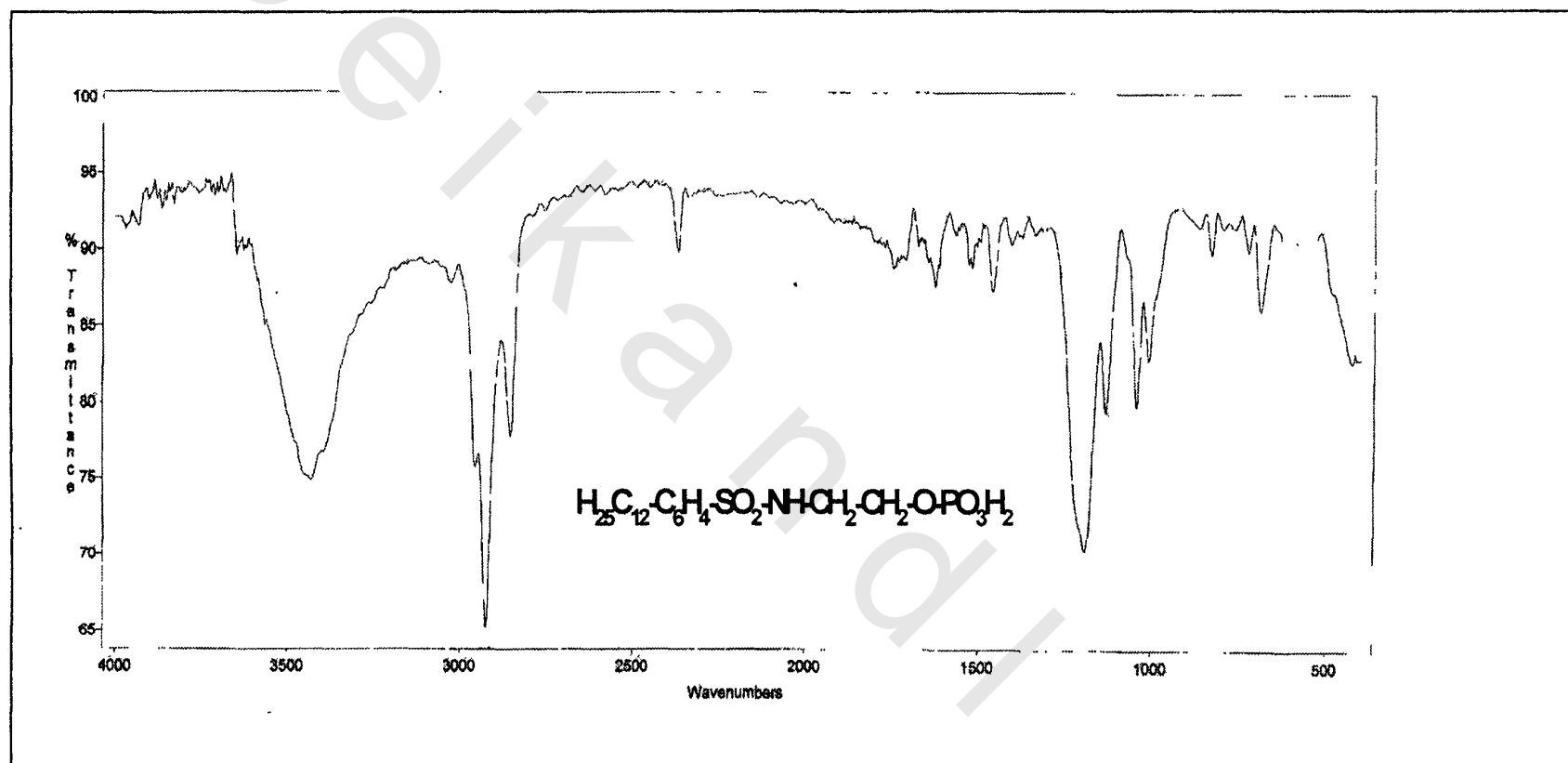


Fig. 12: FT.ir of 4-dodecyl 1-N-ethanol phosphate sulfonamide benzene

III.1.2. Preparation of AFFF Based on Dodecylphenol

Preparation of aqueous film forming foam surfactants based on dodecylphenol has been achieved by acylating phenol, then, reducing the produced lauroylphenol according to Hung-Minlon modification of Wolff-Kischner reduction to produce dodecylphenol. Then, dodecylphenol was ethoxylated as in the experimental section to give 4-dodecylphenol ethoxylate (9). This was followed by either phosphorylation or sulfation to give 4-dodecylphenol polyoxyethylene (9) phosphate and sulfate, respectively.

The FT.ir spectrum of dodecylphenol presented in the corresponding *Fig. 13*, it shows a band at 3087 cm^{-1} characteristic for C-H ring stretching vibration, bands at 2959 and 2871 cm^{-1} assigned for asymmetric and symmetric C-H stretching of linear alkyl part, bands at 1460 and 1374 cm^{-1} characteristic for C-H deformation of CH_2 - and CH_3 - groups respectively, bands at 1611 and 1512 cm^{-1} assigned to C=C ring stretching, a broad band at 3280 - 3550 cm^{-1} characteristic for O-H group, and finally band at 828 cm^{-1} assigned to p-substitution benzene ring.

Fig.14 shows the FT.ir spectrum of 4-dodecylbenzene polyoxyethylene (9). In the spectrum the appearance of a strong broad band at 1110 cm^{-1} indicates the presence of polyoxyethylene, and the band at 3461 cm^{-1} refers to the terminal O-H group of polyoxyethylene, confirms the completion of the ethoxylation reaction.

Fig. 15 shows the FT.ir spectrum of 4-dodecylbenzene polyoxyethylene (9) phosphate, besides the characteristic bands for 4-dodecylbenzene polyoxyethylene (9), the chart shows three bands at 1059, 2320, and 2736 cm^{-1} characteristic for P-OH group, a band at 1244 cm^{-1} characteristic for P=O group, and finally the band at 994 cm^{-1} characteristic for P-O-C group. Also, the disappearance of band at 3461 cm^{-1} refers to the terminal O-H group, all these bands indicate the presence of phosphate group which confirms the phosphorylation reaction.

Fig. 16 shows the FT.ir spectrum of 4-dodecylbenzene polyoxyethylene (9) sulfate, the chart shows the appearance of the characteristic bands for 4-dodecylbenzene polyoxyethylene (9), in addition to a band at 1244 cm^{-1} characteristic for S=O group, and a band at 694 cm^{-1} characteristic for S-O group. These bands are referring to the presence of sulfate group and confirms the sulfation reaction.

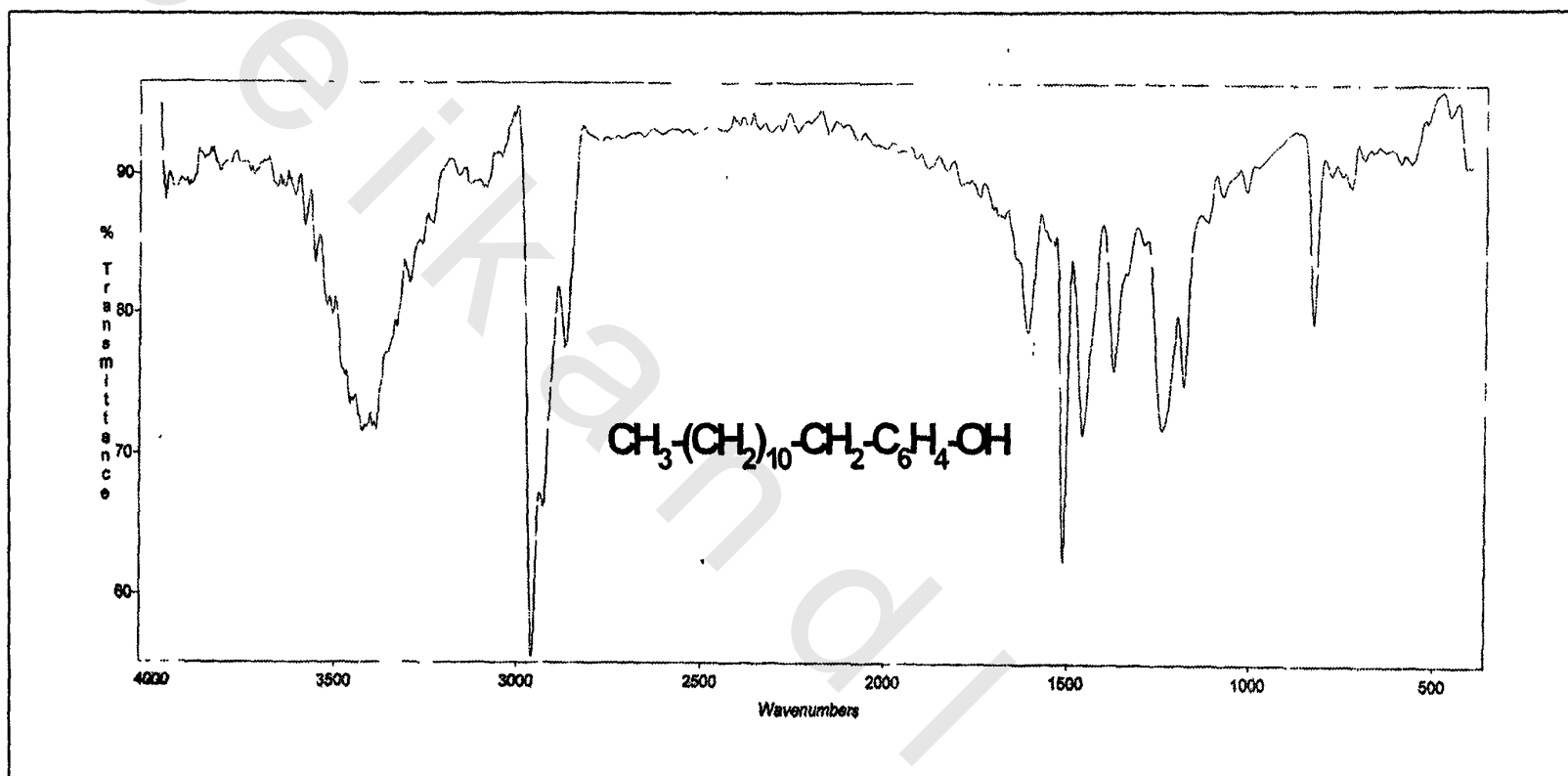


Fig. 13: FT.ir Dodecylphenol

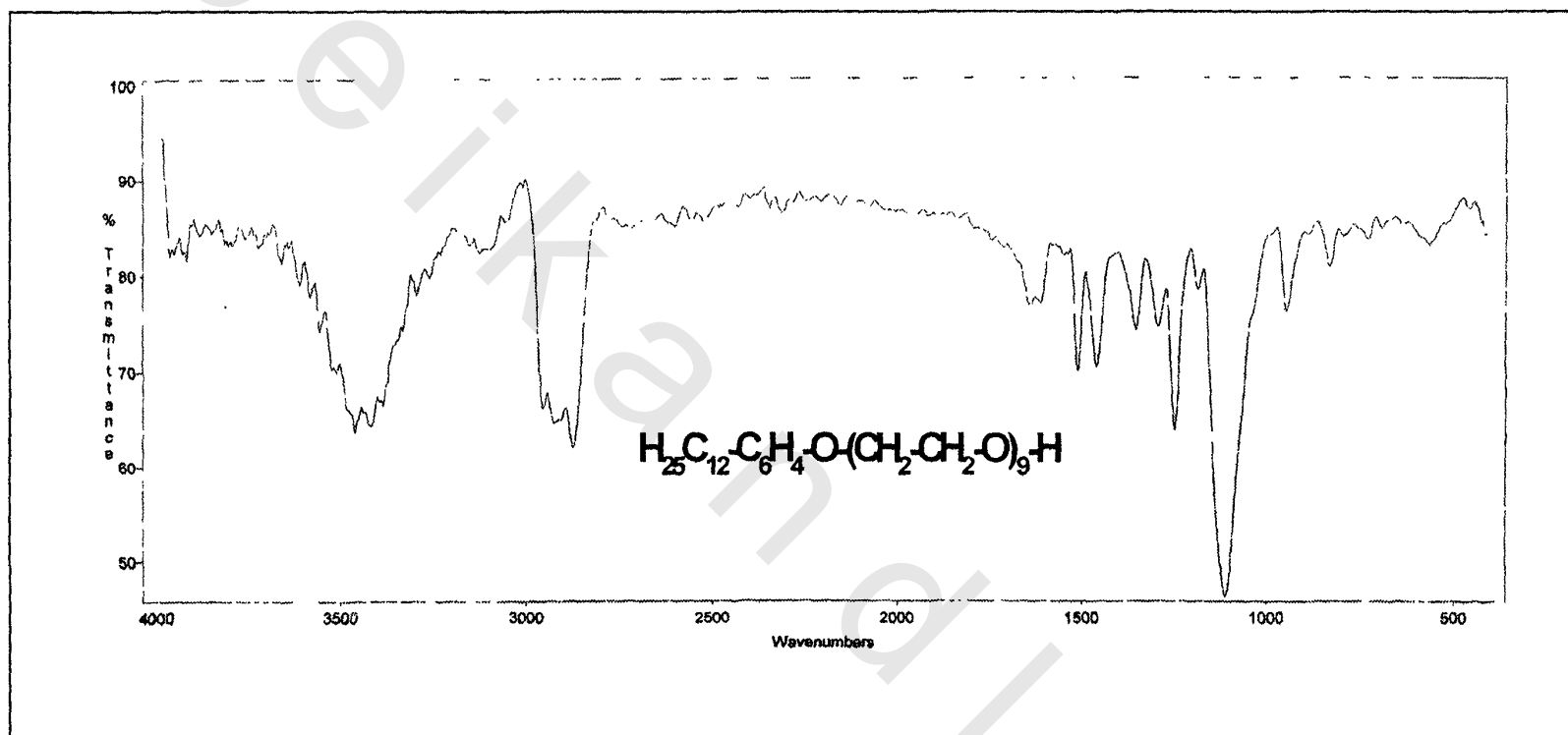


Fig. 14: FT.ir 4-dodecylphenol polyoxyethylene (9)

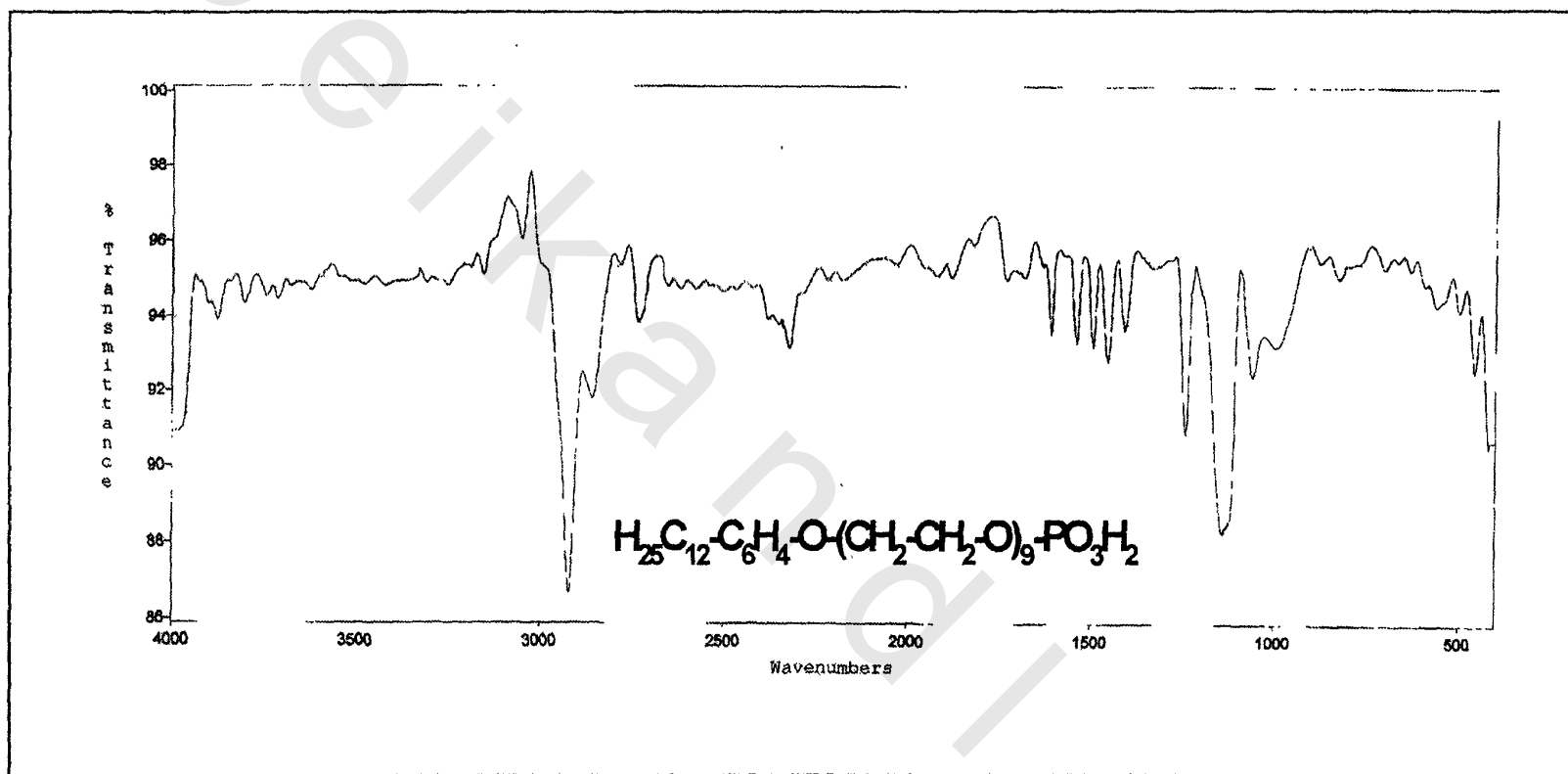


Fig.15: FT.ir of 4-dodecylphenol polyoxyethylene (9) phosphate

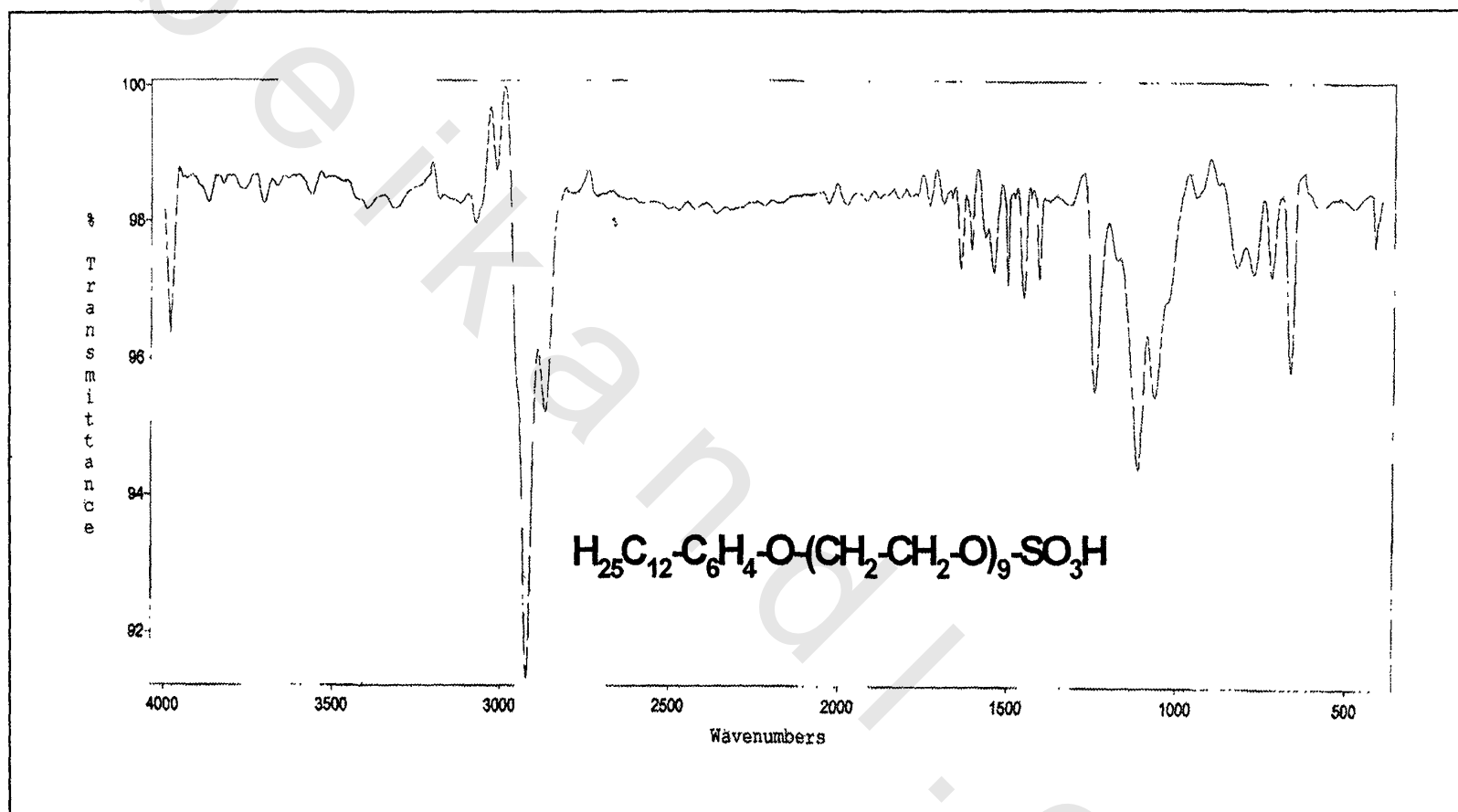


Fig. 16: FT.ir of 4-dodecylphenol polyoxyethylene (9) sulfate

III.2. Surface and Thermodynamic Parameters of The Prepared Surfactants

III.2.1. Surface active properties

Surface tension of the prepared surfactants were measured at 25, 35, and 45°C. The critical micelle concentrations (CMC) of them were determined by plotting surface tension γ versus log solute concentration, C . *Figs 17 to 28* are showing the γ -ln C adsorption isotherms, the values of surface tension at critical micelle concentrations (γ_{CMC}) at 25, 35, and 45°C are listed in *Table 4 (Rosen M., 1976)*, it is shown that the γ_{CMC} values belong to DBMSA(I-b), DBPS(I-e), and DBBS(I-f) are smaller than those belong to DBMSASP(I-g), DBPSSP(I-h), and DBBSSP(I-i), on the other hand, the γ_{CMC} value belong to DPE(II-a) is greater than those belong to DPESP(II-b) and DPESP(II-c). The CMC values were determined from the abrupt change in the slope of γ versus ln C plots. These values are listed in *Table 4*. It is shown from the data that increasing the temperature from 25 to 45°C leads to a decrease in CMC for all derivatives, the CMC values of sodium salts of the phosphorylated sulfonamide, and sulfonates [DBMSASP(I-g), DBPSSP(I-h), and DBBSSP(I-i)] are slightly greater than the corresponding sulfonamide, and sulfonates [DBMSA(I-b), DBPS(I-e), and DBBS(I-f)], this is may be due to the slightly difference in the hydrophilic lipophilic balance (HLB). Also, the CMC values of both sodium salts of phosphorylated and sulfated dodecylphenol ethoxylate [DPESP(II-b) and DPESP(II-c)] are greater than that of dodecylphenol ethoxylate itself, as shown in *Table 4*, this is may be ascribed to the HLB values that are listed also in *Table 4*. The HLB values were

calculated by using the general formula for both anionic and nonionic surfactants (*Griffin W. C., 1954*) ($HLB = \sum \text{hydrophobic group no} + \sum \text{hydrophilic group no} + 7$), ($HLB = 20 \times M_H / (M_H + M_L)$), or ($HLB = eo\% / 5$), where M_H is the formula weight of the hydrophilic portion of the molecule, M_L is the formula weight of the hydrophobic portion, and $eo\%$ is the ethylene oxide percentage. An inspection of *Table 4* indicates that γ_{CMC} increases with the rise in temperature.

Maximum surface excess concentrations (Γ_{max}) in mol dm^{-2} were calculated from the relationships:

$$\Gamma_{max} = 1/RT(-\delta\gamma/\delta\ln C)T$$

Where $(-\delta\gamma/\delta\ln C)T$ is the slope of γ versus $\ln C$ plots at a constant absolute temperature T and $R = 8.314 \text{ J mol}^{-1}\text{k}^{-1}$. The Γ_{max} values were used to calculate the minimum area (A_{min} , in $\text{nm}^2 \text{ molecule}^{-1}$) at the aqueous-air interface using the relationship:

$$A_{min} = 10^{16} / N\Gamma$$

Where, N is Avogadro's number. Values of A_{min} are listed in *Table 4*. A_{min} values increases with rising the temperature from 25 to 45°C. This is probably due to the increased thermal kinetic motion (*Rosen M., et al, 1983 and Teo H., et al, 1984*). The effectiveness of surface tension reduction Π_{CMC} were measured at CMC from the relationship:

$$\Pi_{CMC} = \gamma_0 - \gamma_{CMC}$$

Where γ_0 is the surface tension of water and γ_{CMC} is the surface tension of the solution at CMC. The Π_{CMC} continuously decreases with the rise in temperature.

III.2.2. Thermodynamic Parameters of Micellization and Adsorption

The thermodynamic parameters of micellization are summarized in *Table 5*, these parameters are the standard free energies ΔG_{mic} , enthalpies ΔH_{mic} , and entropies ΔS_{mic} of micellization for the prepared surfactants were investigated:

$$\Delta G_{mic} = RT \ln CMC$$

Values of ΔS_{mic} were obtained from the relationship:

$$-\delta \Delta G_{mic} / \delta T = -\Delta S_{mic}$$

by using the values of ΔG_{mic} at 25, 35, and 45°C. In addition, ΔH_{mic} was calculated from the equation:

$$\Delta H_{mic} = \Delta G_{mic} + T \Delta S_{mic}$$

Analyzing the thermodynamic parameters of micellization, we may conclude that micellization process is spontaneous. The data in *Table 5* reveal that $-\Delta G_{mic}$ increases with increasing temperature from 25 to 45°C, the $-\Delta G_{mic}$ values of both DBPS(I-e) and DBBS(I-f) are greater than the rest of surfactants which indicates that increasing the number of hydrophilic groups (polyoxyethylene and polyoxypropylene) favors the micellization process. The values of ΔS_{mic} that obtained at 25-45°C are all positive, which indicating increased randomness in the system upon transformation of the surfactant molecules into micelles. The ΔH_{mic} values in the *Table 5* are also positive. The thermodynamic parameters of adsorption are summarized in *Table 6*. These parameters are ΔG_{ad} , ΔH_{ad} , and ΔS_{ad} . The ΔG_{ad} values were calculated by using the relationship (*Rosen M., and Aronson S., 1981*):

$$\Delta G_{ad} = RT \ln CMC - 6.023 \times 10^{-1} \Pi_{CMC} A_{CMC}$$

The ΔG_{ad} values are all negative and they are more negative than ΔG_{mic} , this indicates that adsorption process at the interface is associated with a decrease in the free energy of the system. The ΔH_{ad} and ΔS_{ad} values listed in *Table 6* are obtained as before from relationships corresponding to those for ΔH_{mic} and ΔS_{mic} . The ΔS_{ad} values are all positive and slightly greater than the ΔS_{mic} values for the same compounds. This may reflect the greater freedom of motion of the hydrocarbon chains at the planar air-aqueous solution interface compared with that in the relatively cramped interior beneath the convex surface of the micelle. The ΔH_{ad} values are all positive and less than the ΔH_{mic} values.

III.2.3. Structure Effects on Micellization and Adsorption

From the equations that used in calculating ΔG_{mic} and ΔG_{ad} , it follows that:

$$\Pi_{CMC} A_{min} = \Delta G_{mic} - \Delta G_{ad},$$

The $\Pi_{CMC} A_{min}$ product express the work involved in transferring the surfactant molecule from a monolayer at zero surface pressure to the micelle; $\Delta G_{mic} - \Delta G_{ad}$ values are listed in *Table 7*. It is apparent that the work of transfer, which measures the ease of adsorption to form a monolayer at zero surface pressure relative to ease of micellization, shows observed change with temperature in the 25-45°C range, they are all positive values and each value increases with rising temperature. On the other hand, the values of $\Delta H_{mic} - \Delta H_{ad}$ are all positive except that of DPES(II-c), which means a smaller dehydration for the polyoxyethylene chain in the molecule, also the value for DPESP(II-b) is greater than the other

positive values which indicates that a greater dehydration of the molecule is required for micellization than for adsorption at the air-aqueous interface. Also, the values of $\Delta S_{mic} - \Delta S_{ad}$ are all negative values, this may be caused by the great restriction on the motion of the alkyl chain in the relatively cramped interior of the micelle compared with the planer air-aqueous solution interface, as indicated the steric factors inhibit micellization more than they do adsorption at the air-aqueous solution in the interface (*Al Sabagh A. M., 1998*).

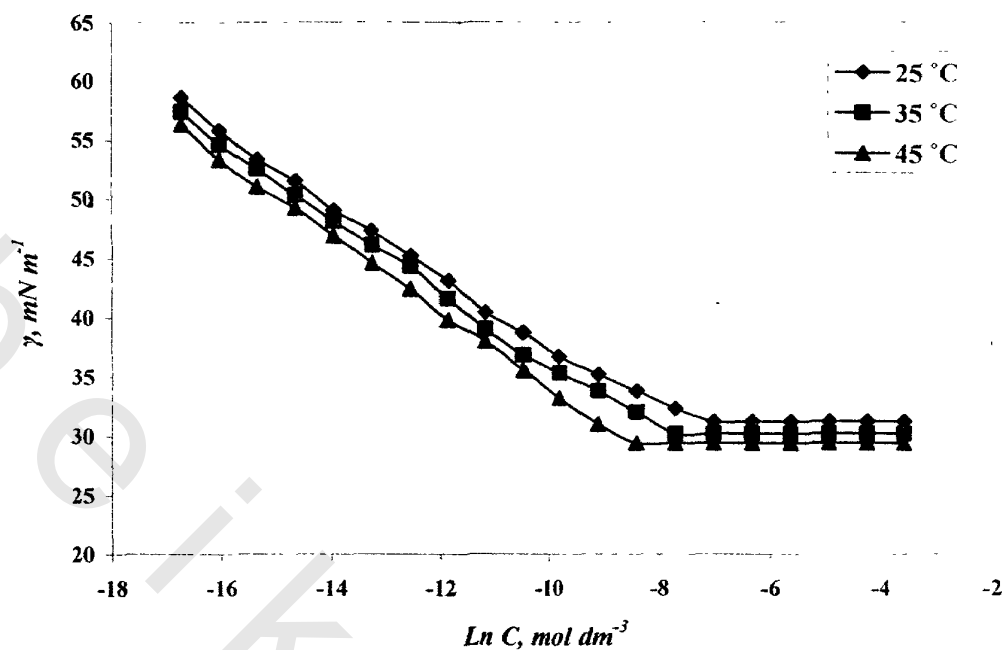


Fig 17: γ -Ln C adsorption isotherm for DBSS

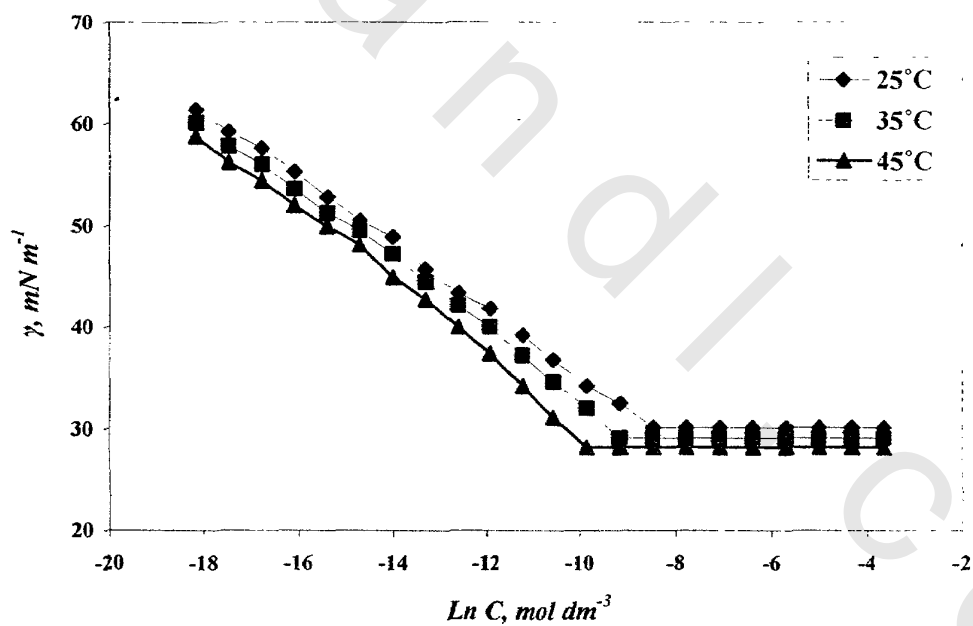


Fig 18: γ -Ln C adsorption isotherm for DBMSA

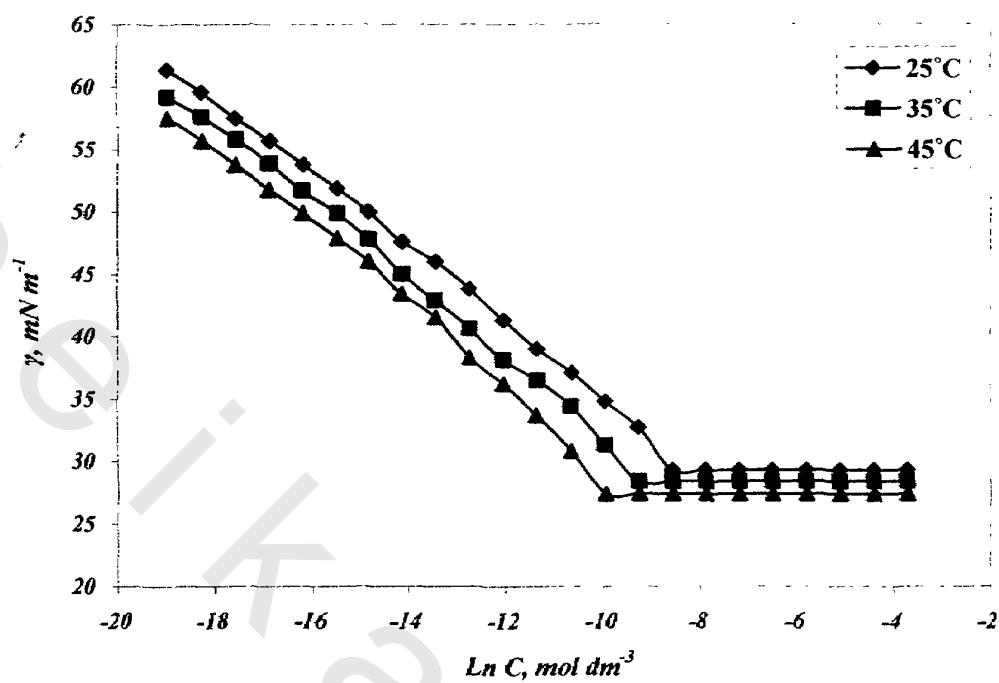


Fig. 19: γ -Ln C adsorption isotherm for DBDSA

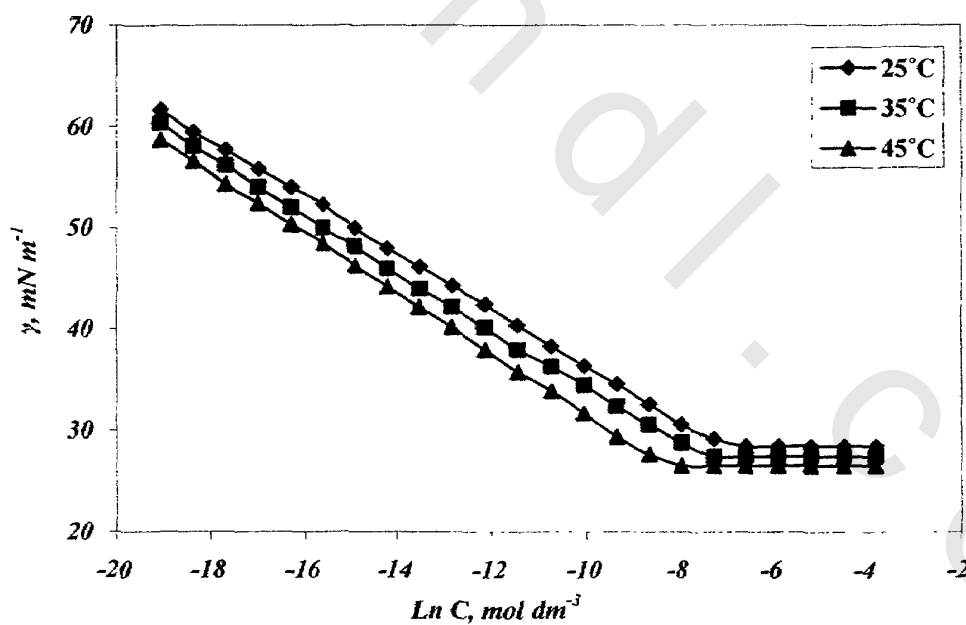


Fig. 20: γ -Ln C adsorption isotherm for DBTS

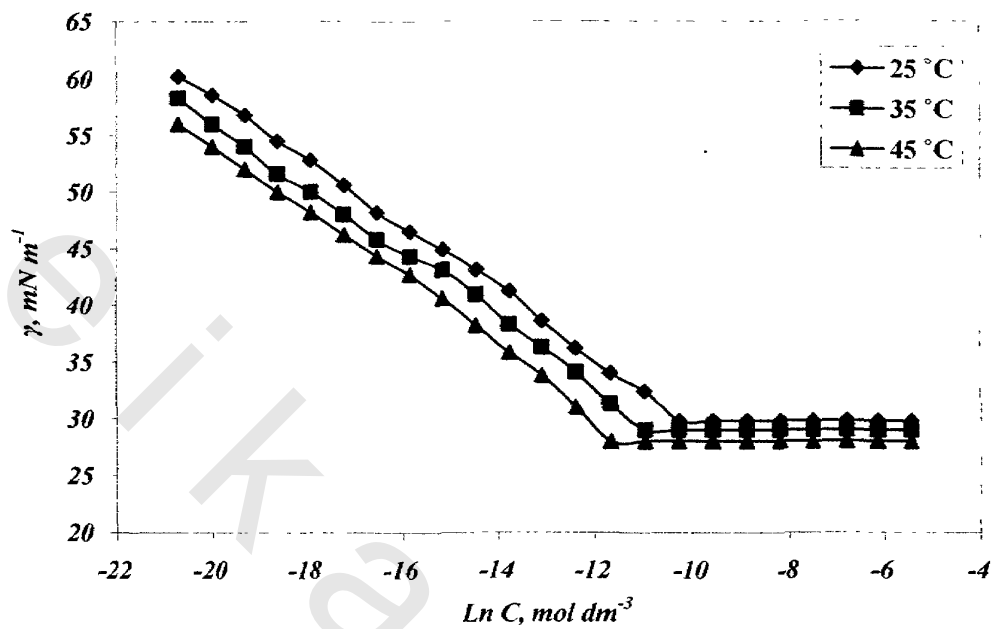


Fig. 21: γ -Ln C adsorption isotherm for DBPS

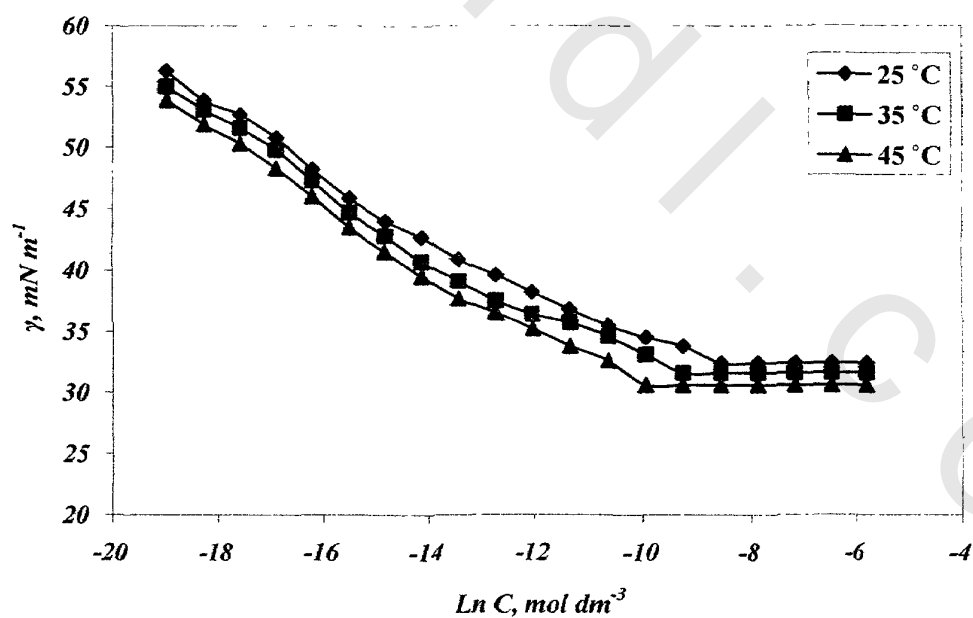


Fig. 22: γ -Ln C adsorption isotherm for DBBS

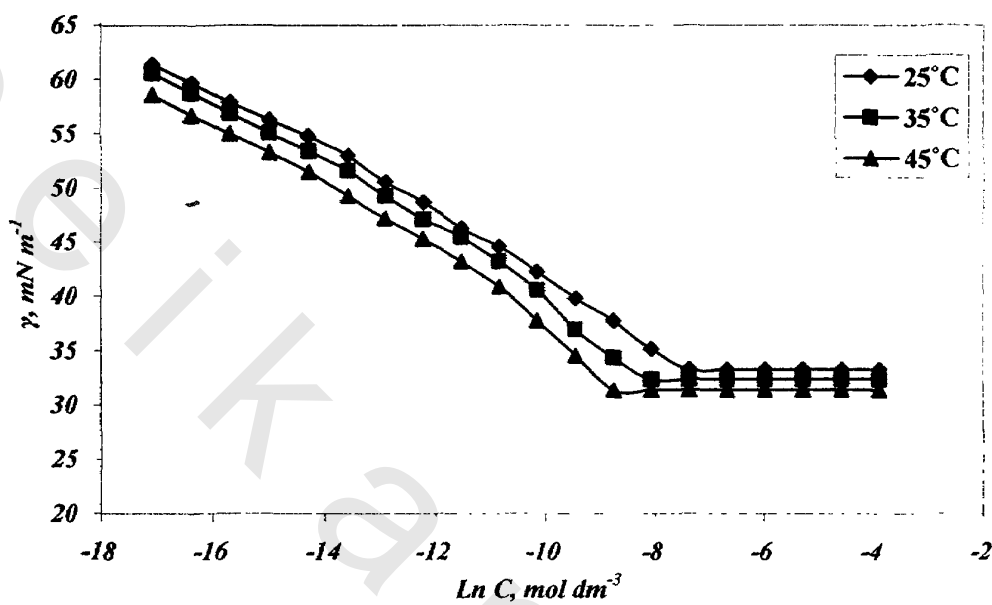


Fig 23: γ - Ln C adsorption isotherm for DBMSASP

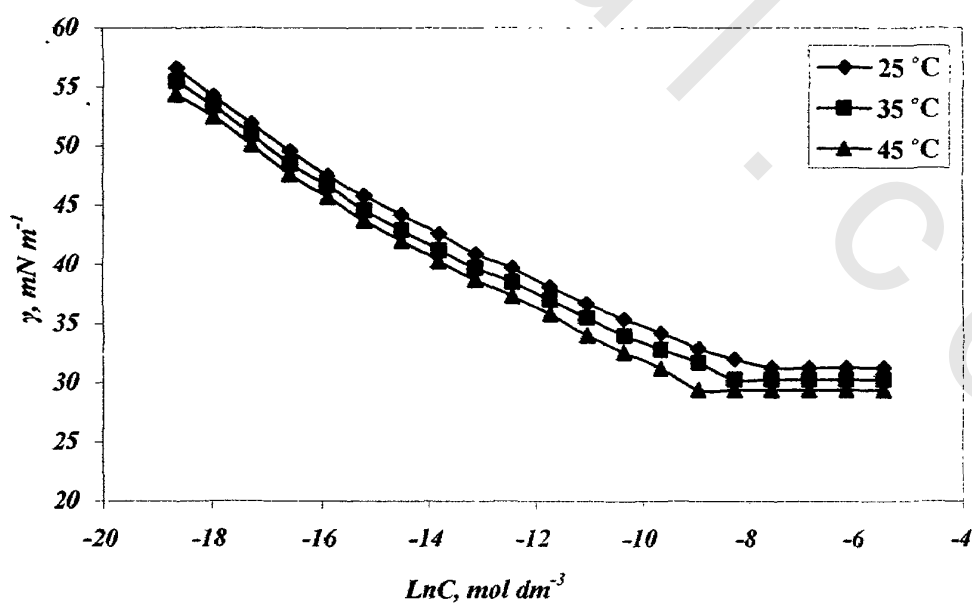


Fig 24: γ - Ln C adsorption isotherm for DBPSSP

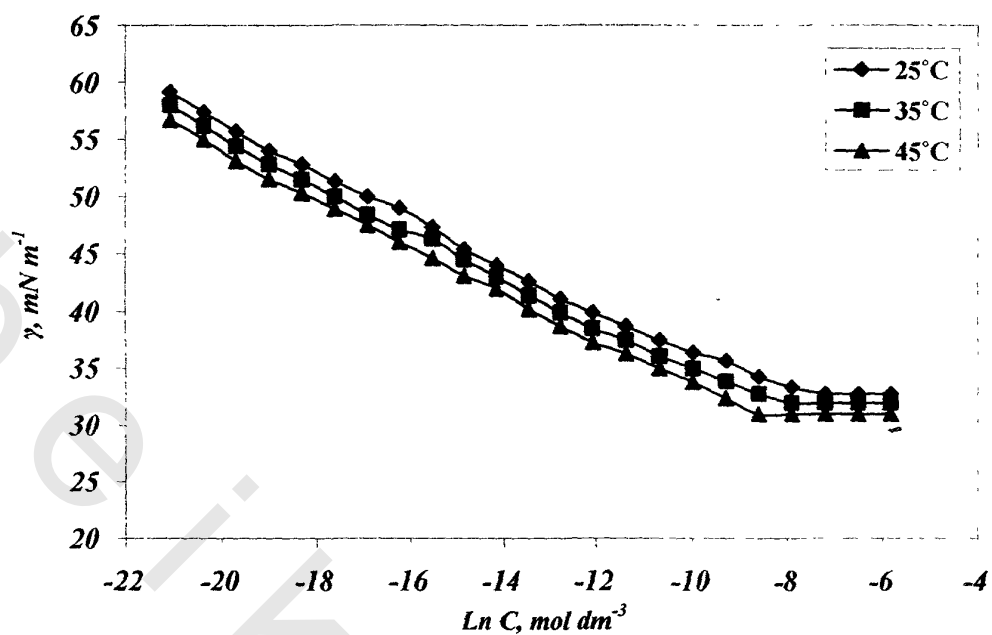


Fig. 25: γ -Ln C adsorption isotherm for DBBSP

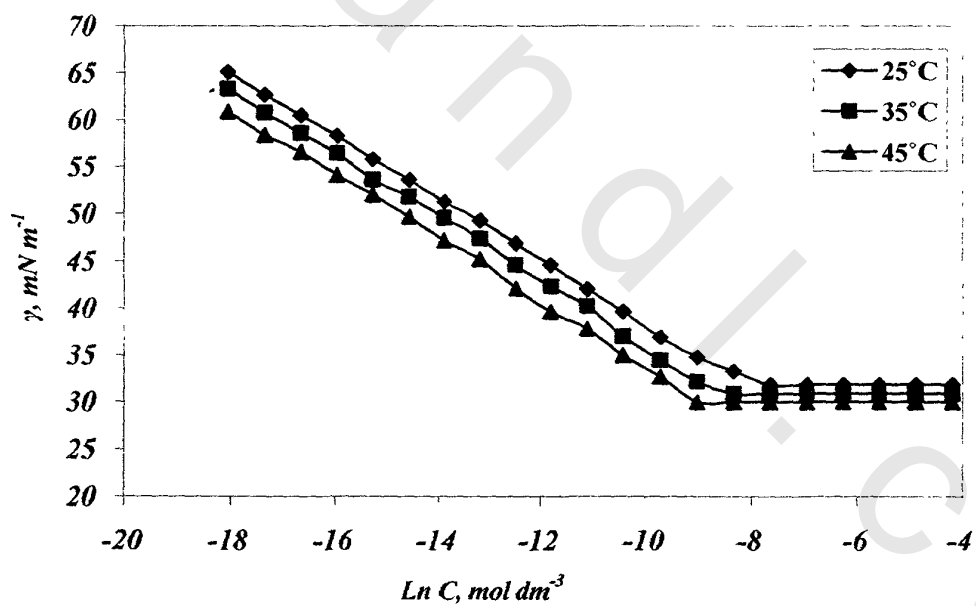


Fig. 26: γ -Ln C adsorption isotherm for DPE

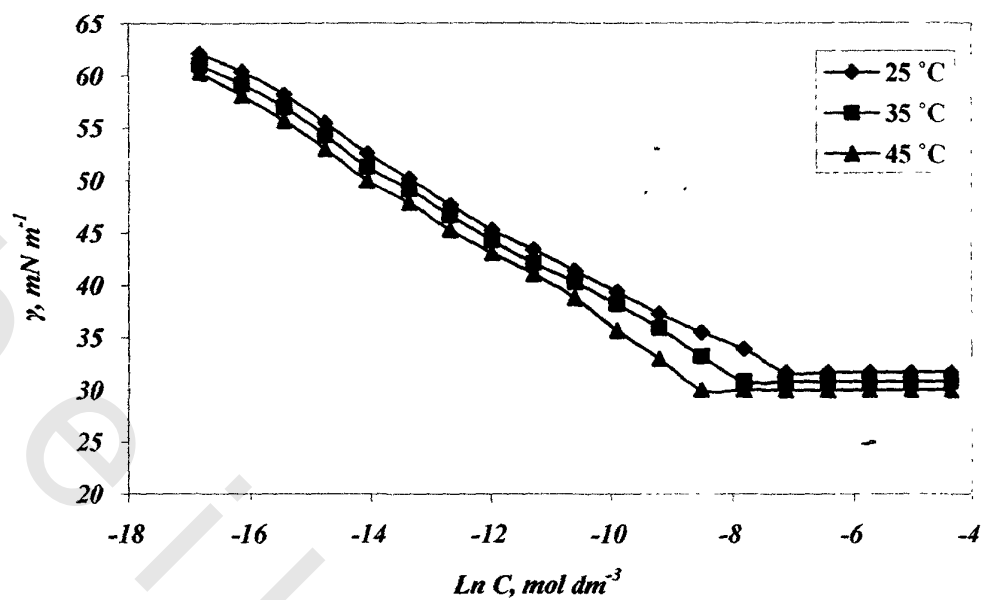


Fig. 27: γ - Ln C adsorption isotherm for DPESP

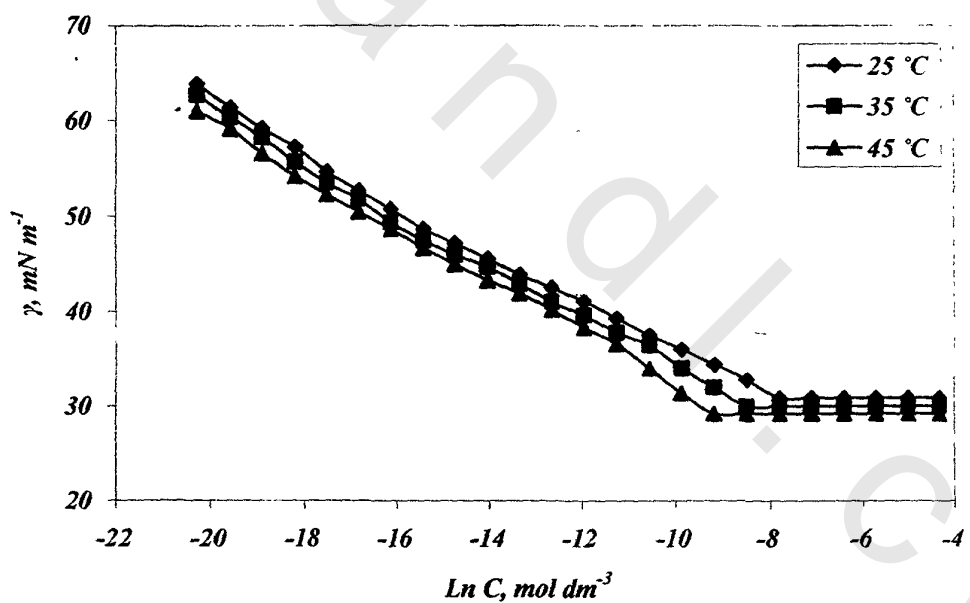


Fig. 28: γ - Ln C adsorption isotherm for DPESP

Table 4: HLB and surface properties of the prepared surfactants

Abb.	HLB	γ_{CMC} (mN m ⁻¹)			CMC $\times 10^{-4}$ (mol. dm ⁻³)			Π_{CMC} (mN m ⁻¹)			$\Gamma_{max}\times 10^{-10}$ (mol. cm ⁻²)			A_{min} (nm molecule ⁻¹)		
		25 °C	35 °C	45 °C	25 °C	35 °C	45 °C	25 °C	35 °C	45 °C	25 °C	35 °C	45 °C	25 °C	35 °C	45 °C
DBSS	10.6	31.2	30.2	29.4	4.54	3.41	1.80	40.8	40.2	39.4	1.25	1.21	1.17	132.6	137.1	141.6
DBMSA	6.7	30.1	29.1	28.2	2.03	1.50	0.83	41.9	41.3	40.6	1.36	1.32	1.28	121.2	125.2	129.4
DBDSA	8.14	29.3	28.4	27.4	3.35	1.52	1.02	42.7	42.0	41.4	1.24	1.20	1.16	133.1	137.5	142.1
DBTS	9.28	28.5	27.5	26.6	7.46	4.53	2.48	43.5	42.9	42.2	1.15	1.11	1.08	143.4	148.3	153.1
DBPS	17.0	29.8	29	28	0.45	0.25	0.16	42.2	41.4	40.8	1.18	1.14	1.10	140.2	144.9	149.6
DBBS	18.0	32.0	31.2	30.2	0.82	0.54	0.33	40.0	39.2	38.6	1.01	0.97	0.94	164.1	169.6	175.1
DBMSASP	10.0	33.3	32.4	31.4	8.20	5.53	4.51	38.7	38.0	37.4	1.21	1.17	1.13	137.1	141.7	146.3
DBPSSP	16.4	31.3	30.3	29.4	2.25	1.64	1.01	40.7	40.1	39.4	0.96	0.93	0.90	171.3	177.1	182.9
DBBSSP	17.5	32.8	32.0	31.0	2.75	1.84	1.66	39.2	38.4	37.8	0.81	0.79	0.76	202.9	209.7	216.6
DPE	12.0	32.4	31.4	30.5	2.74	1.84	1.23	39.6	39.0	38.3	1.37	1.32	1.28	120.9	125.0	129.1
DPESP	10.1	31.7	30.8	30	4.09	3.35	2.48	40.3	39.6	38.8	1.29	1.24	1.21	128.5	132.8	137.2
DPESS	10.4	30.9	30	29.2	3.35	2.25	1.51	41.1	40.2	39.6	1.04	1.01	0.98	158.2	163.5	168.8

Table 5: Thermodynamic parameters of micellization for the prepared surfactants

Abb.	ΔG_{mic} (Kj mol ⁻¹)			ΔH_{mic} (Kj mol ⁻¹)			ΔS_{mic} (Kj mol ⁻¹ K ⁻¹) ($\Delta G/\Delta T$)
	25 °C	35 °C	45 °C	25 °C	35 °C	45 °C	
DBSS	-19.0709	-20.4438	-22.7968	40.2013	40.81743	40.45344	0.1989
DBMSA	-21.0651	-22.5467	-24.8434	39.30973	39.85405	39.5834	0.2026
DBDSA	-19.824	-22.5128	-24.2984	54.5866	54.39477	55.10618	0.2497
DBTS	-17.8405	-19.7165	-21.9495	48.64334	48.99829	48.99632	0.2231
DBPS	-24.7976	-27.1349	-29.1959	47.37796	47.46267	47.82375	0.2422
DBBS	-23.311	-25.1629	-27.2819	41.05704	41.3651	41.40608	0.216
DBMSASP	-17.6061	-19.2057	-20.3684	28.07726	28.01067	28.38105	0.1533
DBPSSP	-20.8101	-22.3183	-24.3245	35.75026	36.14015	36.03193	0.1898
DBBSSP	-20.313	-22.0236	-23.0108	24.83403	24.6384	25.16617	0.1515
DPE	-20.322	-22.0236	-23.8035	36.35761	36.558	36.68014	0.1902
DPESP	-19.3295	-20.4892	-21.9495	36.63489	37.35317	37.77092	0.1878
DPESS	-19.824	-21.5085	-23.2612	22.4622	22.19673	21.86298	0.1419

Table 6: Thermodynamic parameters of adsorption of the prepared surfactants

Abb.	ΔG_{ad} (Kj mol ⁻¹)			ΔH_{ad} (Kj mol ⁻¹)			ΔS_{ad} (Kj mol ⁻¹ K ⁻¹) ($\Delta G/\Delta T$)
	25 °C	35 °C	45 °C	25 °C	35 °C	45 °C	
DBSS	-22.3311	-23.7639	-26.1564	38.60095	39.2129	38.86502	0.20447
DBMSA	-24.1238	-25.6628	-28.0061	37.97942	38.52445	38.2651	0.2084
DBDSA	-23.2471	-25.9927	-27.84	53.09755	52.91378	53.62842	0.25619
DBTS	-21.5994	-23.5479	-25.8408	47.0777	47.43374	47.44549	0.23046
DBPS	-28.3613	-30.7483	-32.8726	45.66491	45.76194	46.12179	0.24841
DBBS	-27.2639	-29.1667	-31.3524	39.01433	39.33559	39.37397	0.22241
DBMSASP	-20.8016	-22.4487	-23.6638	26.57744	26.52024	26.89502	0.15899
DBPSSP	-25.0109	-26.596	-28.664	33.85306	34.2432	34.15051	0.19753
DBBSSP	-25.1043	-26.8746	-27.941	22.28071	22.10049	22.62415	0.15901
DPE	-23.2071	-24.9604	-26.7812	35.01314	35.21361	35.34648	0.19537
DPESP	-22.4491	-23.6575	-25.1546	21.22576	21.48298	21.45149	0.14656
DPESS	-23.7398	-25.467	-27.2873	34.00669	34.21721	34.33479	0.19378

Table 7: Structural Effects on Micellization and Adsorption

Abb.	$\Delta G_{mic}-\Delta G_{ad}$ (Kj mol ⁻¹)			$\Delta H_{mic}-\Delta H_{ad}$ (Kj mol ⁻¹)			$\Delta S_{mic}-\Delta S_{ad}$ (Kj mol ⁻¹ K ⁻¹) ($\Delta G/\Delta T$)
	25 °C	35 °C	45 °C	25 °C	35 °C	45 °C	
DBSS	3.2601	3.3199	3.3594	1.60035	1.60453	1.58842	-0.00557
DBMSA	3.0588	3.1158	3.1631	1.33031	1.3296	1.3183	-0.0058
DBDSA	3.4231	3.4797	3.542	1.48905	1.48099	1.47776	-0.00649
DBTS	3.7584	3.8309	3.8908	1.56564	1.56455	1.55083	-0.00736
DBPS	3.5633	3.6133	3.6766	1.71305	1.70073	1.70196	-0.00621
DBBS	3.9529	4.0037	4.0704	2.04271	2.02951	2.03211	-0.00641
DBMSASP	3.1956	3.2427	3.2958	1.49982	1.49043	1.48603	-0.00569
DBPSSP	4.2009	4.278	4.339	1.8972	1.89695	1.88142	-0.00773
DBBSSP	4.7913	4.8506	4.93	2.55332	2.53791	2.54202	-0.00751
DPE	2.8851	2.9364	2.9772	1.34447	1.34439	1.33366	-0.00517
DPESP	3.1191	3.1685	3.2046	15.40913	15.87019	16.31943	0.04124
DPESS	3.9158	3.958	4.0263	-11.5444	-12.0205	-12.4718	-0.05188

III.3. Foam performance of the prepared surfactants

III.3.1. Foam properties and Sealability of the prepared surfactants

A fire fighting foam is obtained by dilution of a foam concentrate in water (generally 10% foam concentrate v/v). This water/foam concentrate mixture is called a foaming solution or premix (*Garcia G., 1994*). The foaming base of a foam concentrate consists of either a mixture of hydrocarbon surfactants (foaming agents), foam stabilizer (ethylene glycol butyl ether), and reducer interfacial tension agent (sodium dioctyl sulfosuccinate). The typically synthetic foam concentrate designed to be diluted from 10% to 6, 3, and 1%. High performance foam concentrates that are of interest here contain different hydrophilic parts, which play an important role in the formation of the foam as well the formation of a water film at the surface of the solvent (cyclohexane). *Tables 8 to 11* show some foam properties of the prepared surfactants. By inspection the presented data it was found that, DBSS(I-a), DBBS(I-f), DBMSASP(I-g), DBPSSP(I-h), DBBSSP(I-i), DPESP(II-b), and DPESP(II-c) failed to form film of sealability (stable foam). These surfactants gave unstable foam film in spite of forming foams. They have high surface potential electric double layer on the surface of foam lamellae, on the each side of the foam thin film the interfacial charge will be equal. If a foam film is stabilized by ionic surfactants then, their presence at the interfaces will induce a repulsive force that opposes the thinning process. The magnitude of the force will depend on the charge density and the film thickness. Having a charged interface influences the distribution of the

nearby ions in a polar medium. Ions of opposite charge (counterions) are attracted to the surface, while those of like charge (coions) are repelled. An electric double layer, which is diffuse because of mixing caused by thermal motion, is thus formed. The electrical double layer consists of the charged surface and a neutralizing excess of counterions over coions, distributed near the surface.

The presence of mixed surfactants adsorption seems to be a factor in obtaining films with very viscous surfaces (*Clunie J. S., et al, 1971*). For example, in some cases the addition of a small amount of nonionic surfactants to a solution of anionic surfactants can enhance foam stability (*Ross S., and Morrison I. D., 1988 and Ross S., 1980*).

The foam stability of gas bubbles and the liquid films between them would be stabilized entirely by the repulsive forces created when two charged interfaces approach each other and their electric double layers overlap. When the two interfaces that bind a foam lamella are electrically charged the interacting diffuse double layers exert a hydrostatic pressure that acts to keep the interfaces apart. In the electrostatic, dispersion, and steric forces all may be significant, and the disjoining pressure concept is frequently employed. The disjoining pressure represents the net pressure difference between the gas phase (bubbles) and the bulk liquid from which the lamellae extend (*Derjaguin B. V., et al, 1987*).

The foam film stability is completely related with concentration of the foaming material solutions. The success foaming solutions in the sealability test was obtained with DBMSA(I-b), DBDSA(I-c), DBTS(I-d), DBPS(I-e), and

DPE(II-a) at concentrations above the CMC. The same solutions gave rupturing foam films at CMC concentrations and below CMC as reported before (*Rusanov A. I., et al, 2004*).

Surfactants bubbles and films have been the focus of scientific interest. The stability and structure of foams are determined primarily by the relative rate of coalescence of the dispersed gas bubbles (*Mckendrick C. B., et al, 1991*). The process of coalescence of foams is controlled by the thinning and rupture of foam films separating the air bubbles. Experimental observations suggest that the lifetime (stability) of foam films is determined primarily by the thinning time rather than by the rupture time. Hence, if the approaching bubbles have equal size the process of coalescence can be split into three stages; 1- formation of a thick lamella; 2- thinning of the lamella to a film by forming spots, the film may reduce its thickness by a single thickness transition when the spots form in the thinning film at low surfactant concentration (below the CMC), or multiple the thickness at concentrations several times higher than the CMC; 3- ruptures according to (*Vrij A., 1966*) due to an unbounded increase in the surface corrugations with time. However, very thin Newton film ruptures because of nucleation (hole formation) according to (*Derjaguin B. V., and Gutop V. V., 1962 and Derjaguin B. V., and Prokhorov A. V., 1981*).

The thermodynamic properties of liquid films are different from those of the bulk surfactant solutions. These films possess an excess chemical potential that is manifested as an excess pressure named as disjoining pressure (*Derjaguin B.*

V., and Kusakov M. M., 1936). Generally the disjoining pressure consists of electrostatic repulsion forces between the two overlapping surface double layers, the attractive van der Waals forces among all molecules of the film, the steric forces due to steric hindrance in closely packed monolayers and in the presence of micelles. When the foam lamella thinned to a thickness of few micelles diameters further thinning occurred in a stepwise manner as the micelles left the film layer by layer. The process of foam lamella thinning is shown in *Fig. 29*. The photomicrographs shown in this figure depict the manner in which the stepwise thinning process occurs (*Srivastava V. J., et al, 2003*). The surface tension of the successful surfactants in the sealability test [DBMSA(I-b), DBDSA(I-c), DBTS(I-d), DBPS(I-e), and DPE(II-a)]. The successful surfactants in the sealability test reduced the surface tension greater than the unsuccessful surfactants as clearly shown in *Table 4*. The foaming agent is needed to reduce surface tension and thereby aid in the formation of the increased interfacial area with a minimum of mechanical energy input and it may be needed to form a protective film at the bubbles surfaces that acts to prevent coalescence with other bubbles. Foams are thermodynamically unstable the term stable is used to mean relatively stable in a kinetic sense. It is important to distinguish the degree of change and the time scale. From thermodynamic principles, surface tension has units of energy per unit area and this illustrates the fact that area expansion of the surface requires energy. Physically surface tension is viewed as the sum of the contracting forces that act parallel to the surface or interface.

Table 8: Foam properties of foam concentrates* (FC 10%).

Foam Concentrates (FC)	Sealability Test with screen	Sealability Time /min	25% Drainage Time /sec	25% Drainage Volume /ml	Expansion Ratio (ER)
DBSS	RF	-	210	4	6.3
DBMSA	SF	2	195	4	5.9
DBDSA	SF	1.5	180	5	5.3
DBTS	SF	2.5	170	5	4.8
DBPS	SF	3.5	165	5.5	4.4
DBBS	RF	-	150	6	4
DBMSASP	RF	-	135	6.5	3.7
DBPSSP	RF	-	120	7	3.6
DBBSSP	RF	-	105	7.5	3.2
DPE	SF	2	120	7	3.5
DPESP	RF	-	105	8	3.13
DPESS	RF	-	150	5.75	4.2

Foam concentrate (FC 10%): is produced by dissolving 10 gm of the prepared surfactant in 100 ml water
RF means rupturing foam, and **SF** means stable foam.

Table 9: Foam properties of 6% premix solutions*:

Foam Concentrates (FC)	Sealability Test with screen	Sealability Time /min	25% Drainage Time /sec	25% Drainage Volume /ml	Expansion Ratio (ER)
DBSS	RF	-	180	4.5	5.6
DBMSA	SF	3	165	4.5	5.3
DBDSA	SF	2	150	5	4.8
DBTS	SF	2	135	5.5	4.4
DBPS	SF	2.5	130	6	4
DBBS	RF	-	120	6.5	3.7
DBMSASP	RF	-	110	7	3.5
DBPSSP	RF	-	105	8	3.13
DBBSSP	RF	-	97.5	8.5	2.9
DPE	SF	1.5	105	8	3.18
DPESP	RF	-	96	9	2.7
DPESS	RF	-	126	6.5	3.8

6% premix solution is produced by adding 6 ml of foam concentrate to 94 ml of water.

Table 10: Foam properties of 3% premix solutions*.

Foam Concentrates (FC)	Sealability Test with screen	Sealability Time /min	25% Drainage Time /sec	25% Drainage Volume /ml	Expansion Ratio (ER)
DBSS	RF	-	150	5	5
DBMSA	SF	3.5	135	5.5	4.6
DBDSA	SF	2.5	120	6	4.3
DBTS	SF	1.5	110	6.5	4
DBPS	SF	1.5	110	7	3.6
DBBS	RF	-	105	7	3.5
DBMSASP	RF	-	100	8	3.03
DBPSSP	RF	-	96	9	2.8
DBBSSP	RF	-	85	9.5	2.6
DPE	SF	1	90	9	2.8
DPESP	RF	-	75	10	2.5
DPESS	RF	-	105	7	3.5

3% premix solution is produced by adding 3 ml of foam concentrate to 97 ml of water.

Table 11: Foam properties of 1% premix solutions.*

Foam Concentrates (FC)	Sealability Test with screen	Sealability Time /min	25% Drainage Time /sec	25% Drainage Volume /ml	Expansion Ratio (ER)
DBSS	RF	-	90	8	3.13
DBMSA	SF	4	85	8.5	2.9
DBDSA	SF	3	67.5	9	2.7
DBTS	SF	1	60	9.5	2.6
DBPS	SF	1	57.3	10	2.5
DBBS	RF	-	52.5	10.75	2.4
DBMSASP	RF	-	50	11	2.3
DBPSSP	RF	-	49.3	11.5	2.2
DBBSSP	RF	-	34.1	12.5	2
DPE	SF	0.5	37.5	11.75	2.13
DPESP	RF	-	31.2	13	1.9
DPESS	RF	-	54	10.5	2.4

1% premixed solution is produced by adding 1 ml of foam concentrate to 99 ml of water.

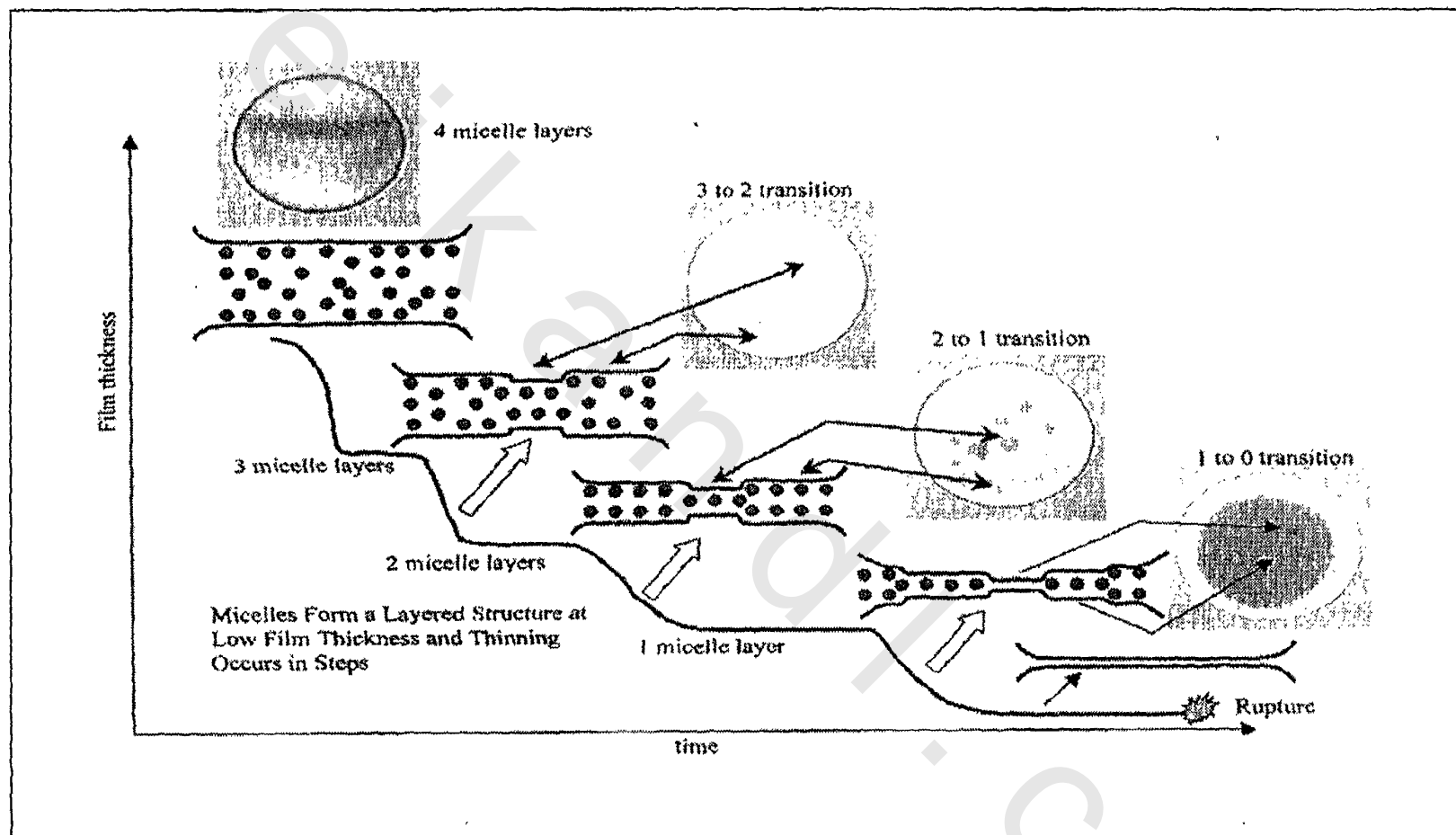


Fig. 29: Schematic sketch of the Change of Film Thickness

The stability of foam is determined by a number of factors involving both bulk solution and interfacial properties such as gravity, drainage, capillary suction, surface elasticity, viscosity of bulk and surface, electric double layer repulsion, dispersion force attraction and steric repulsion. When surfactants concentrate in an adsorbed monolayer at a surface the interfacial film may provide a stabilizing influence in thin films and foams because they can both lower interfacial tension and increase the interfacial viscosity. Increased interfacial viscosity provides a mechanical resistance to foam film thinning and rupturing. A foam film must be somewhat elastic in order to be able to withstand deformations without rupturing. The surface chemical explanation for film elasticity comes from Marangoni and Gibbs (*Adamson A. W., 1982*). Many surfactant solutions showed dynamic surface tension behavior. That is some time is required to establish the equilibrium surface tension. If the surface area of the solution were suddenly increased or decreased, then the adsorbed surfactant layer at the interface would require some time to restore its equilibrium surface concentration by diffusion of surfactant from or to the bulk liquid. In the meantime, the original adsorbed surfactant layer is either expanded or contracted, because the surface tension gradients are now in effect, Gibbs-Marangoni forces arise and act in opposition to the initial disturbance. The dissipation of surface tension gradients in the foam lamellae to achieve equilibrium embodies the interface with a finite elasticity. This fact explains why some substances that lower surface tension do not stabilize foams (*Ross S., and Morrison I. D., 1988*). From

the relation between volumes of drained foam (ml) for different concentrations and the time taken, the 25% drainage time can be calculated as illustrated in *Figs. 30 to 41*.

The increase of 25% drainage time is pointed to the foam stability. Further more the surfactant solution which gives a small time to drain 25 % of foam volume has a low tendency to translate from foam phase to liquid phase. DBSS failed in the sealability test but exhibited the greatest time of 25% drainage time (210 sec) at 10 % surfactant solution. This may be due to its foams had a drop size distribution that is large bubbles (did not pass from the screen mesh). The increase of surfactant concentrations increases the 25% drainage time as shown in *Fig. 42* for all investigated solutions. The increasing of concentrations decreases the 25% drainage volume (ml) as shown in *Fig. 43*. The foam expansion ratio is the ratio between foam volume (aerated) and foam solution (liquid). The foam expansion is increased by increasing foam concentrations as shown in *Fig. 44*. After foam generation, there will always be a tendency for liquid to drain due to the force of gravity. The liquid will drain by flowing downward through the existing liquid films, the interior of the lamellae. Eventually the gas bubbles will no longer be even approximately spherical and relatively planar lamellae will separate polyhedral-shaped bubbles. At this point the capillary forces will become competitive with the forces of gravity. *Fig. 45* shows an additional pressure variation between the Plateau borders (P_B), where the radius of curvature is relatively small (R_{1B}), and in the more laminar part of the lamella (P_A), where the radius of curvature is relatively large (R_{1A}). The principal

radii of curvature have been assumed to be equal at a given location in the lamella. The liquid flow, in response to the pressure difference expressed by Young-Laplace equation which known as Laplace flow or capillary flow. At the Plateau borders (P_B) the gas-liquid interface is quite curved and this curve generates a low gas pressure region (P_G) in the Plateau area. Because the interface is flat along the thin film region, a higher pressure resides there. This pressure difference forces liquid to flow toward the Plateau borders and causes thinning of the films and motion in the foam. This thinning process will lead to film rupture and cause foam collapse and drain.

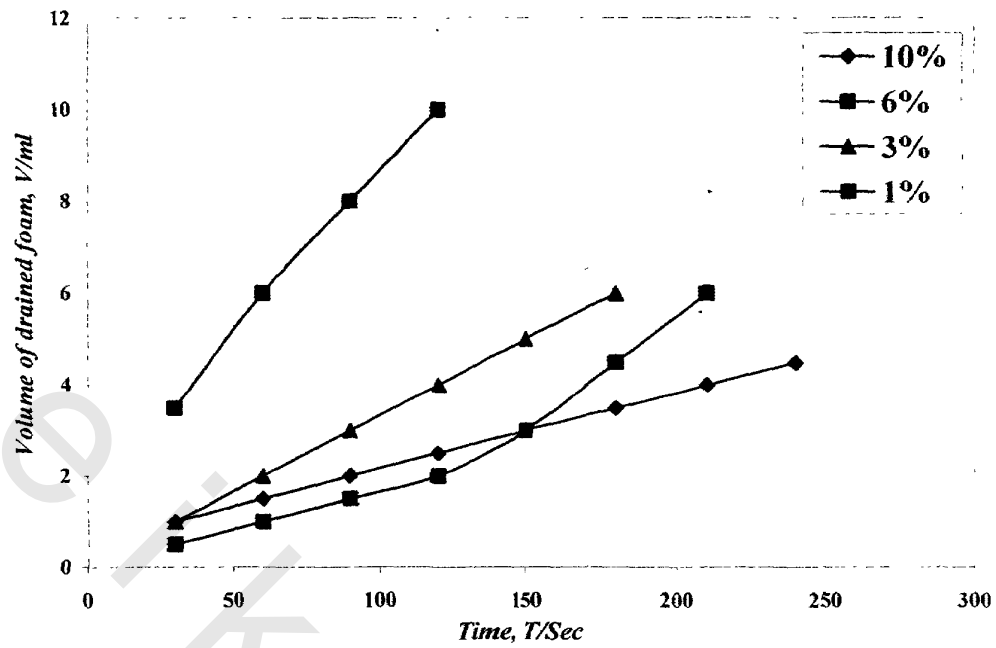


Fig. 30: Relation between 25% drainage volume and time for DBSS

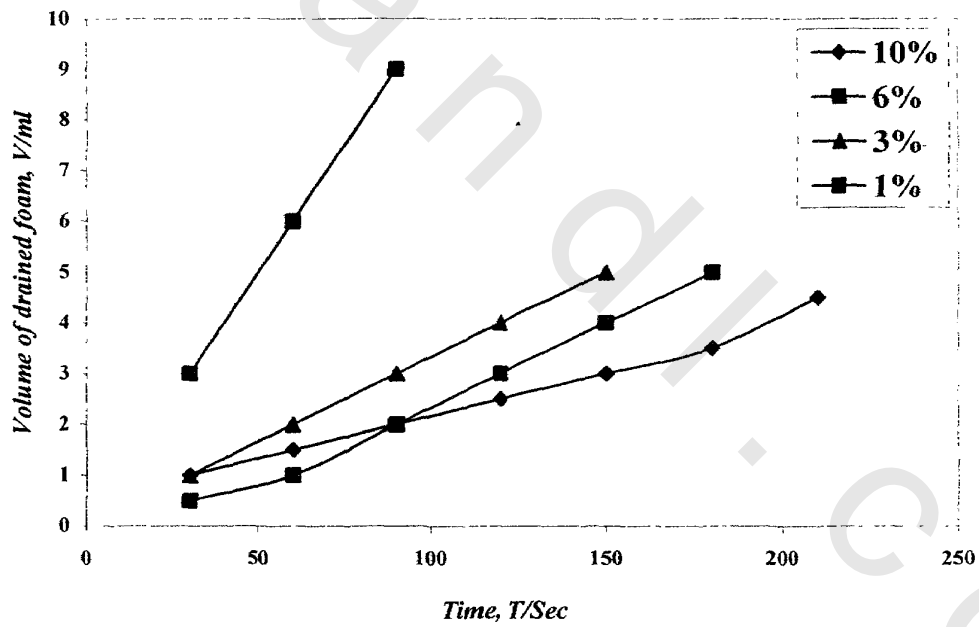


Fig. 31: Relation between 25% drainage volume and time for DBMSA

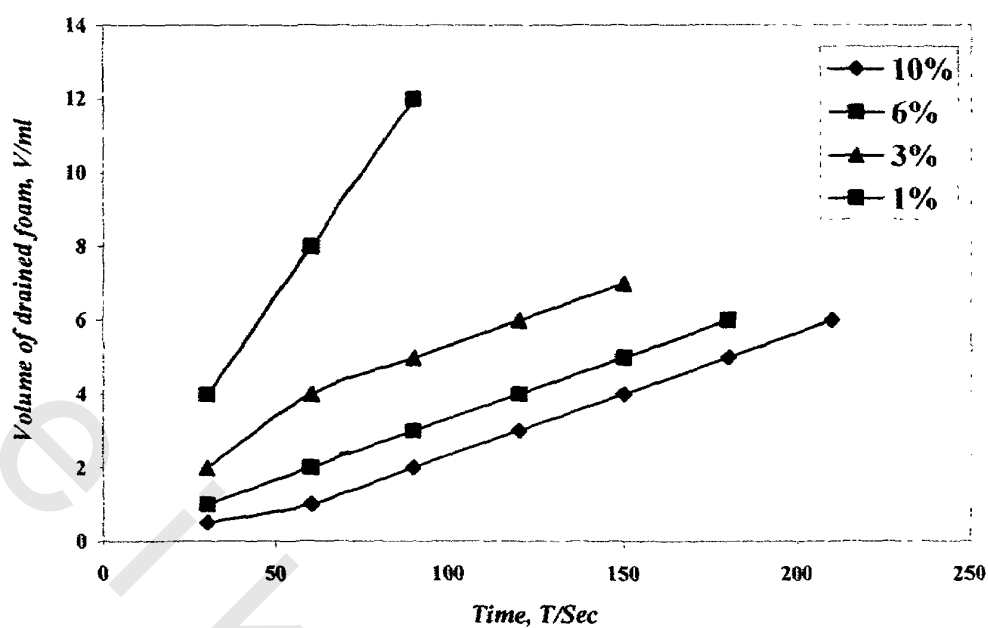


Fig. 32: Relation between 25% drainage volume and time for DBDSA

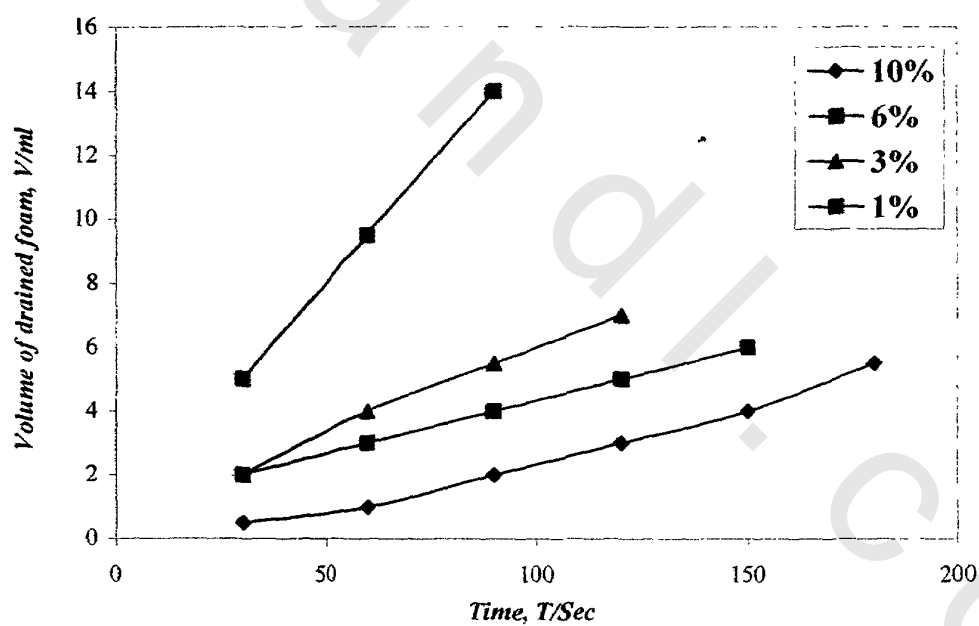


Fig. 33: Relation between 25% drainage volume and time for DBTS

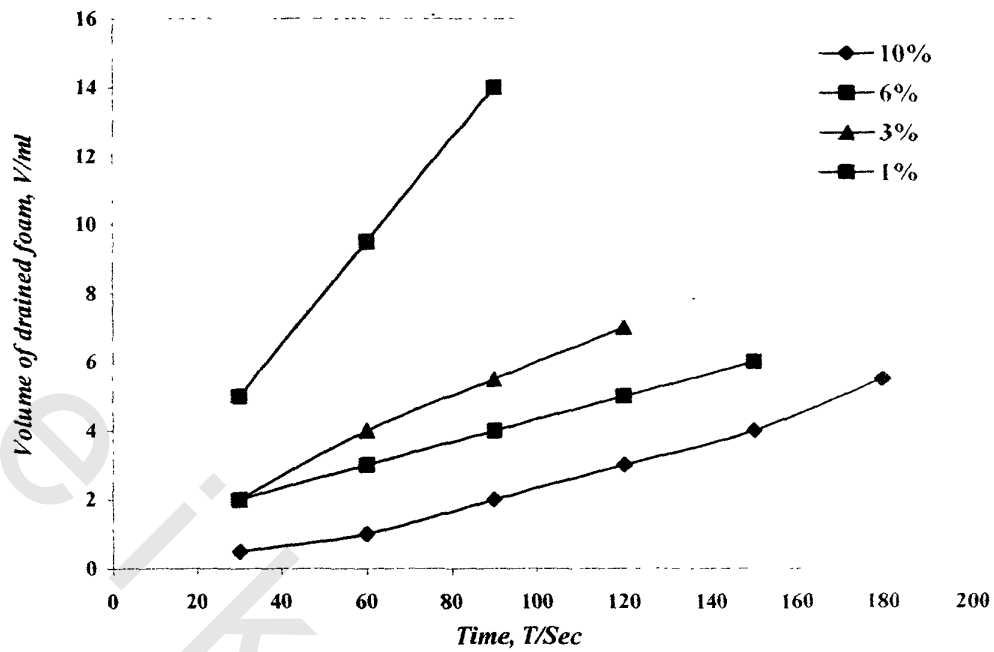


Fig. 34: Relation between 25% drainage volume and time for DBPS

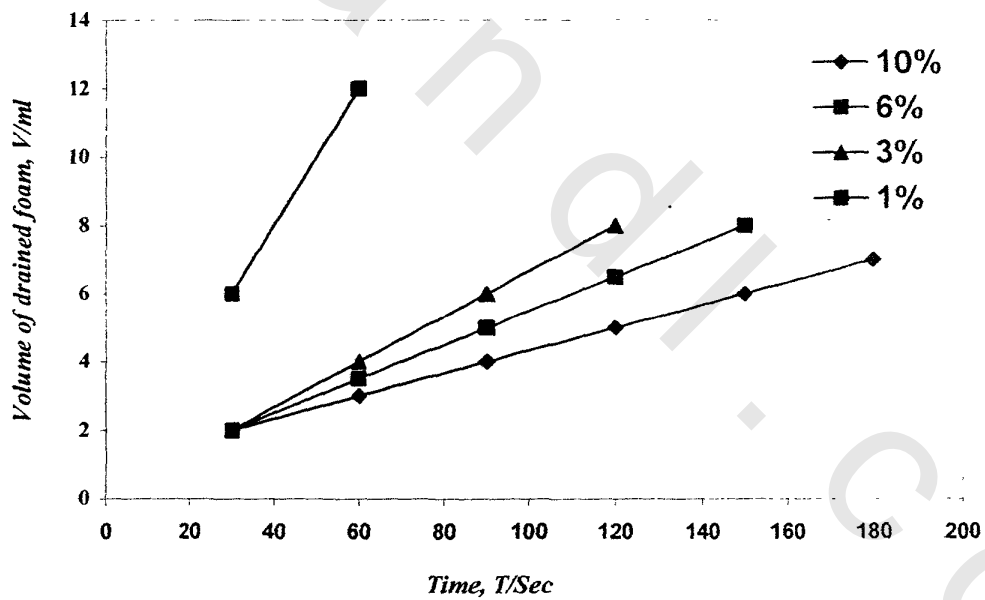


Fig. 35: Relation between 25% drainage volume and time for DBBS

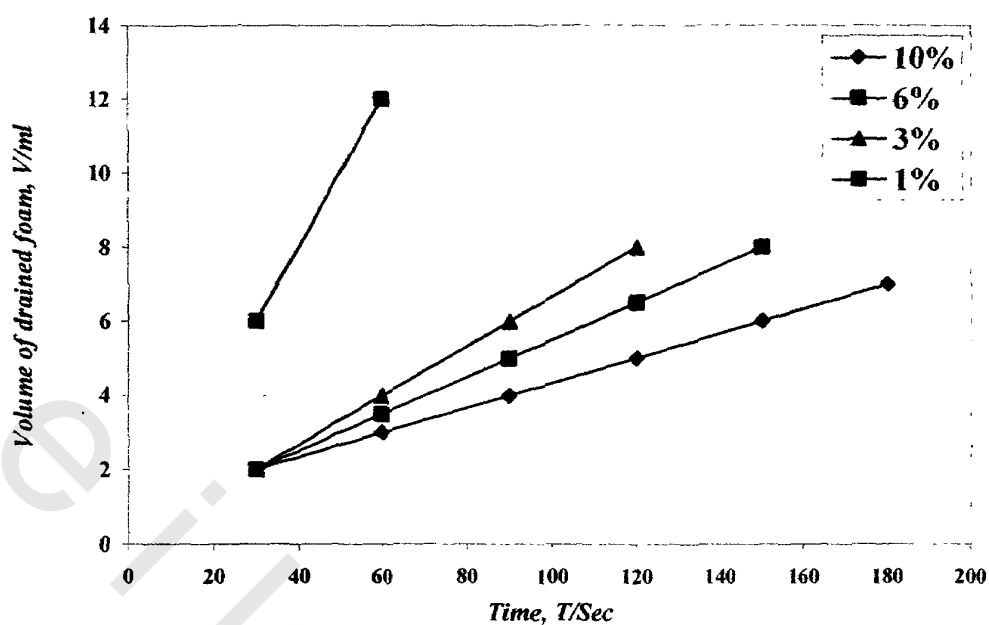


Fig. 36: Relation between 25% drainage volume and time for DBMSASP

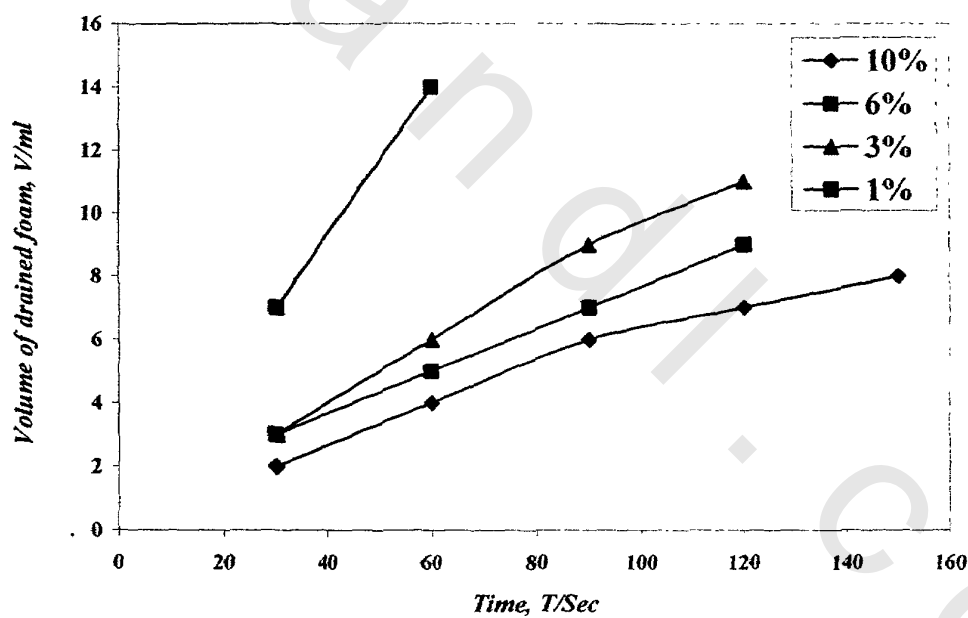


Fig. 37: Relation between 25% drainage volume and time for DBPSSP

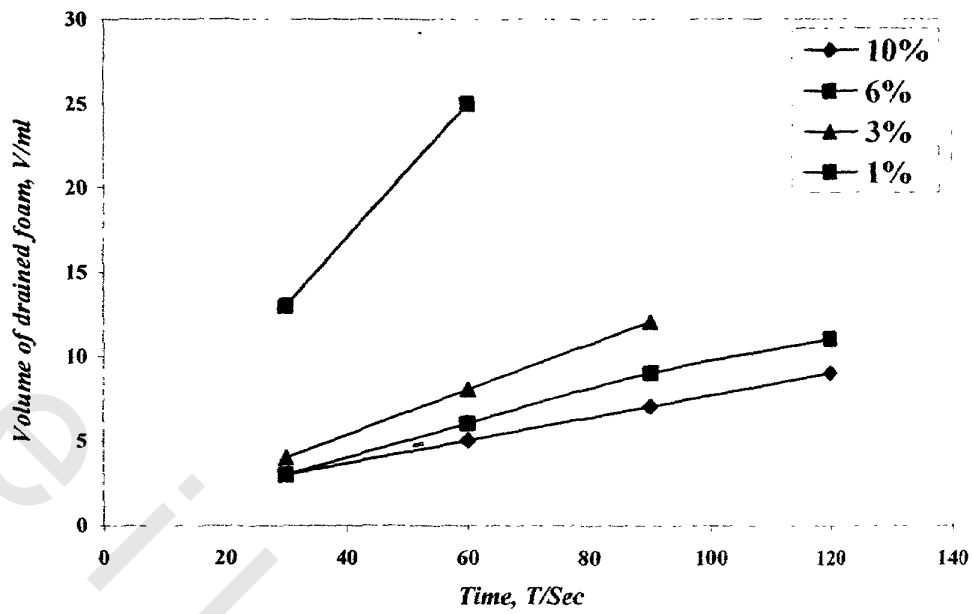


Fig. 38: Relation between 25% drainage volume and time for DBBSP

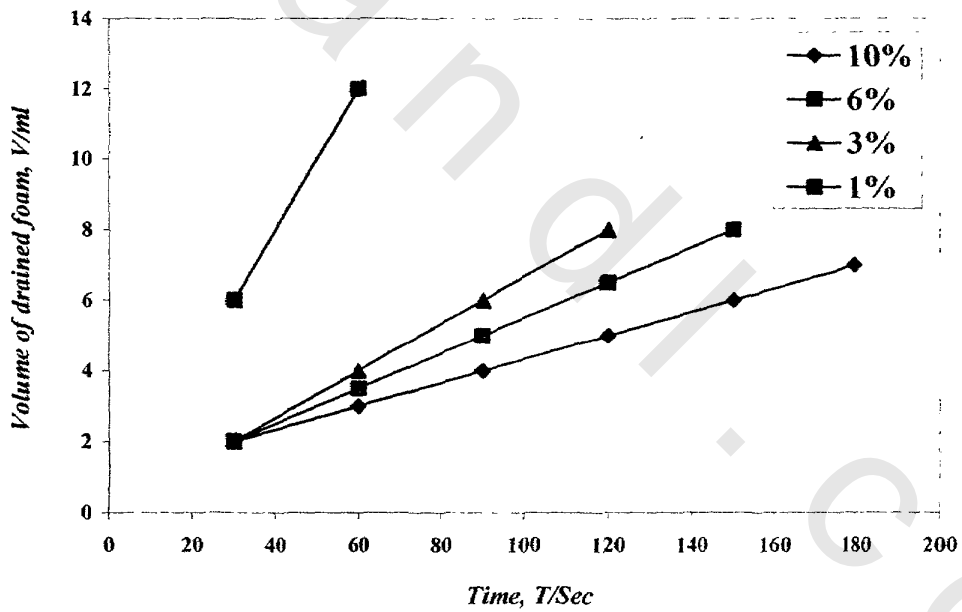


Fig. 39: Relation between 25% drainage volume and time for DPE

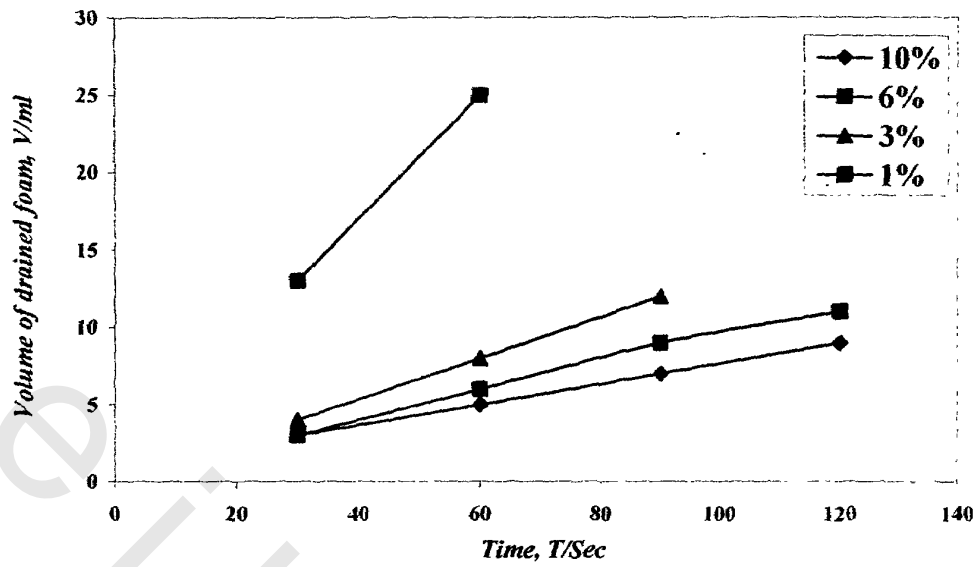


Fig. 40: Relation between 25% drainage volume and time for DPESP

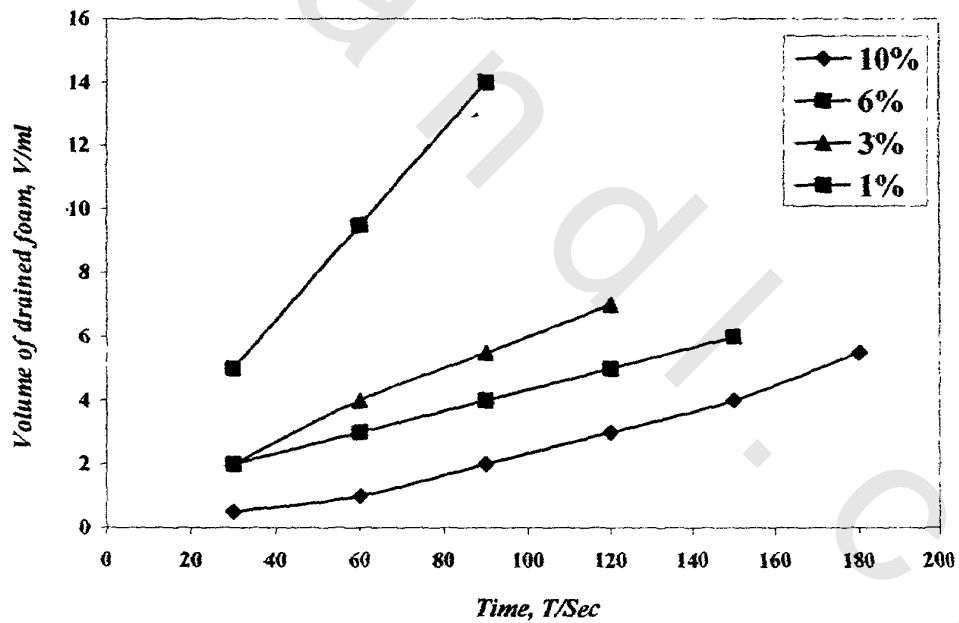


Fig. 41: Relation between 25% drainage volume and time for DPESP

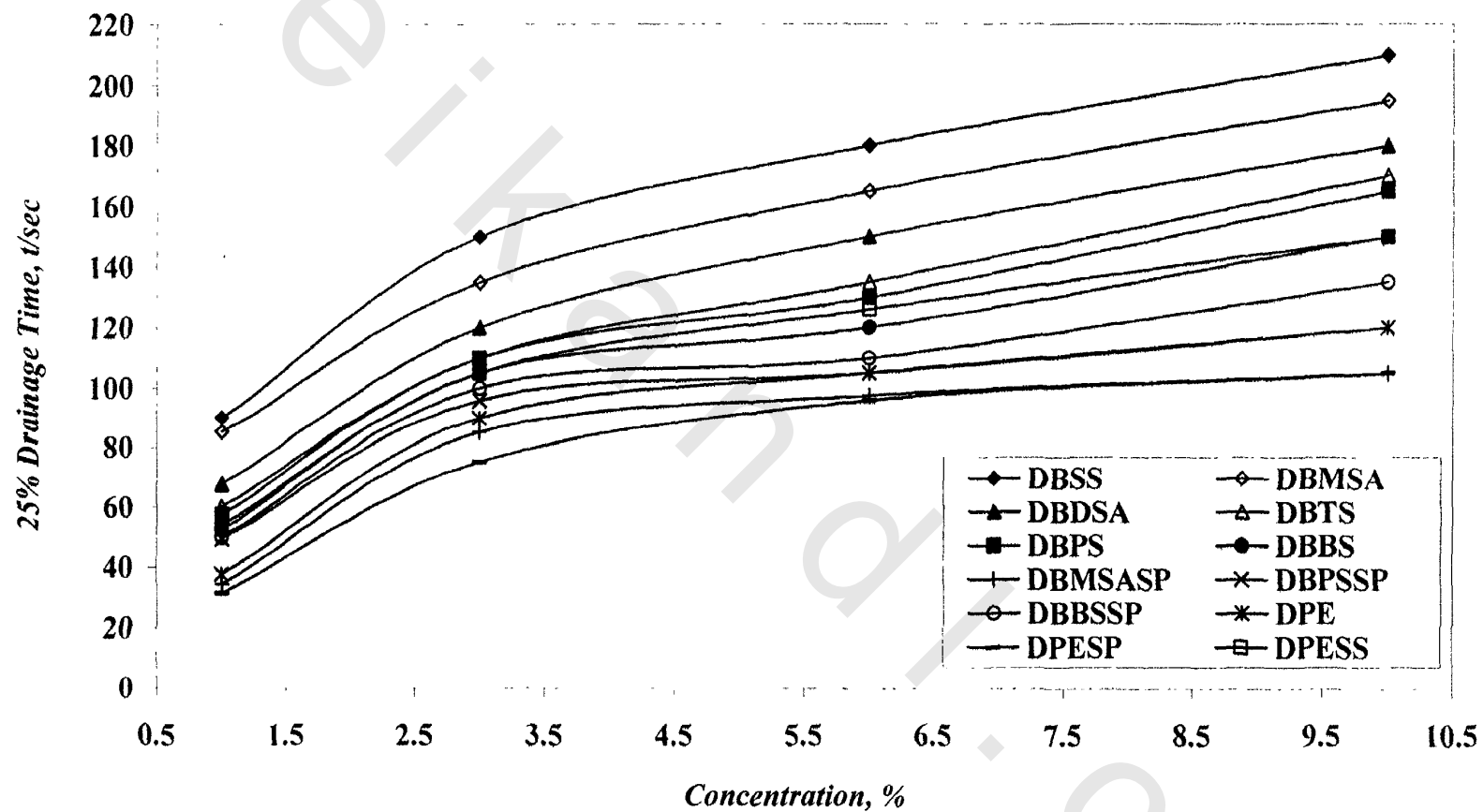


Fig. 42: Relation Between Surfactants Concentrations and 25% Drainage Time.

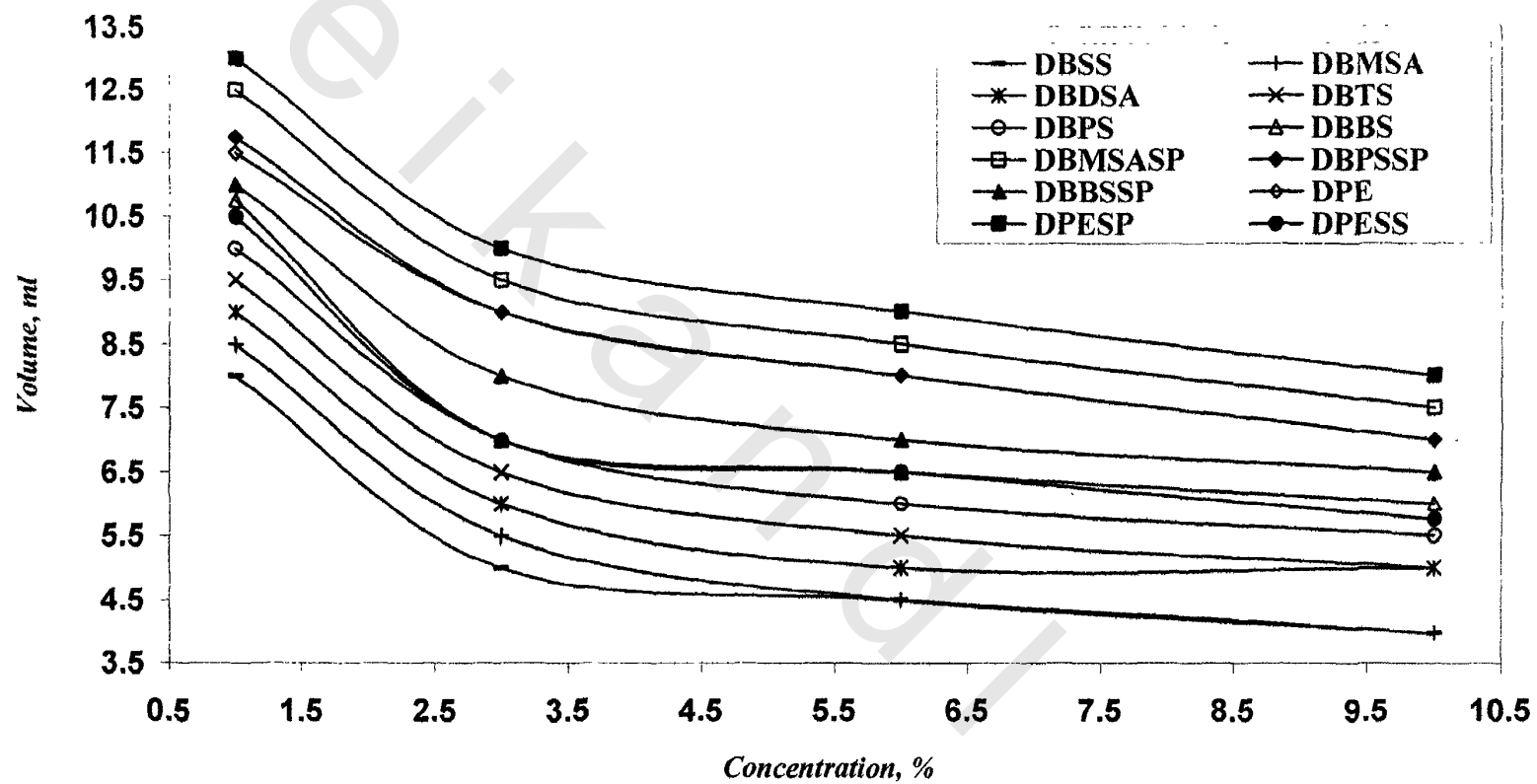


Fig. 43: Relation Between Surfactants Concentrations and Volume of 25% Drainage Time.

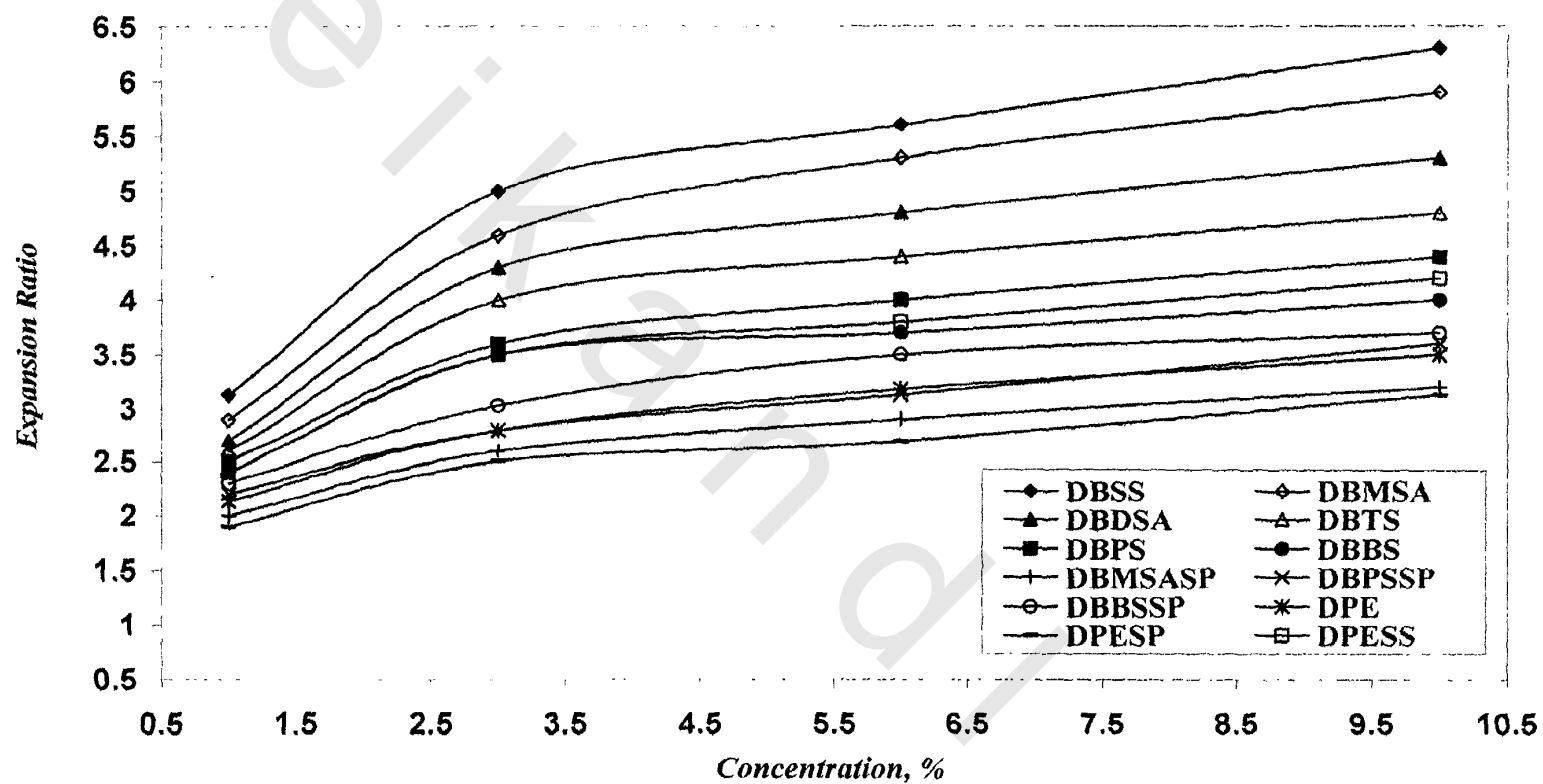


Fig. 44: Relation Between Surfactants Concentrations and Expansion Ratio.

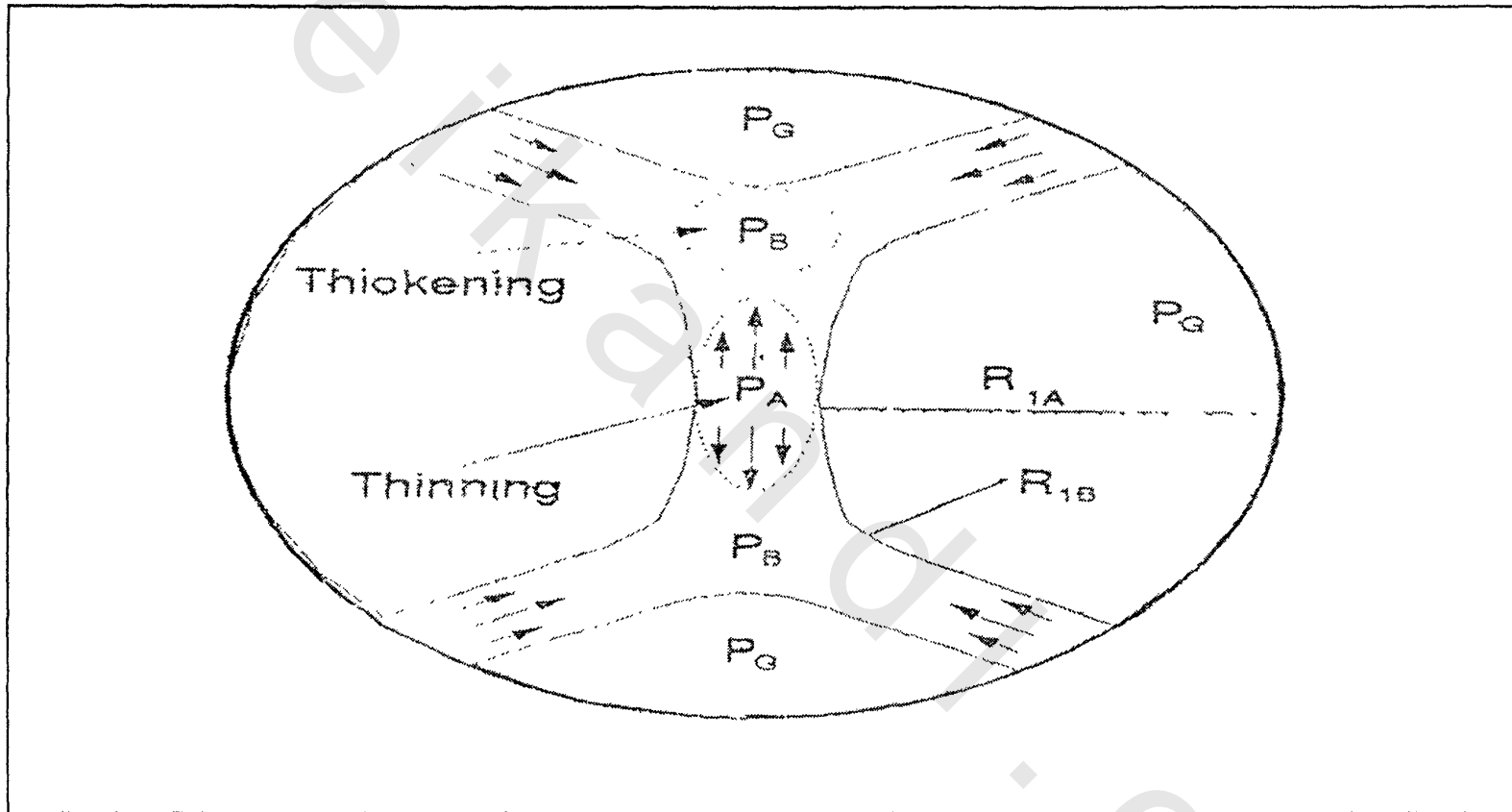


Fig. 45: Pressure Difference across Curved Surfaces in a Foam Lamella

III.3.2. Effect of pH, NaCl, and organic additives on foam properties and sealability

The effect of pH on foam properties of the best surfactant [DBMSA(I-b)] at which the maximum sealability and foam stability were obtained. These properties were measured at different concentration (1, 3, 6, and 10% surfactant concentrations). The pH was changed in the range 2 to 10. From the presented data, it was found that no effect of changing pH on the foaming properties of this surfactant (time of sealability, expansion ratio, and 25% drainage time) as clear in *Table 12*, this may be due to that [DBMSA(I-b)] has nonionic moiety further no ionic strength. The effect of pH on the equivalent film thickness and foam stability appears at certain ionic strength by adding the electrolyte to the nonionic foam system, so that the influence of pH on the electrostatic repulsion of foam bubbles and film thickness is observed at the highest ionic strength by adding the electrolyte (*Sedev R., and Exerowa D., 1999*).

The effect of NaCl on foam properties of DBMSA(I-b) is clearly seen in *Table 13*. By increasing of NaCl concentration, the time of sealability decreases at 1% from 4 to 3 minutes regarding to the sealability film stability. But the same compound did not exhibit sealability at NaCl concentration 2, and 3%. This behavior reflected on the expansion ratio and 25% drainage time that decreased with increasing of NaCl concentration as shown in *Table 13*. This may be due to the electrolyte increases the ionic strength which increases the repulsion ability of the foam bubbles and the film thickness which leads to foam rupture (*Sedev R., and Exerowa D.,*

1999). Also electrolytes do have a weak effect on surface tension, which in the majority of cases is to slightly increase it, due to their desorption from the low-dielectric-constant air phase.

Table 14 clears a comparison between currently used (AFFF) was submitted from Qarun Petroleum Company and three selected individually surfactants [DBMSA(I-b), DBTS(I-d) and DBSS(I-a)] without organic additives. The prepared three surfactants were formulated by organic additives to become as AFFF formulations as shown in *Table 15*. From the presented data, it was found that the organic additives enhanced the sealability time of DBMSA(I-b) and DBTS(I-d) from 3 and 2 (without additives) to 4 and 3 minutes (with organic additives) respectively. This result also reflected on the expansion ratio and the 25% drainage time, which were enhanced after adding the organic additives, from *Tables 14 and 15* the drainage time were 165, 135, and 180 sec against the DBMSA(I-b), DBTS(I-d), and DBSS(I-a) (individual surfactants without organic additives). Meanwhile by addition of the organic additives (formulation as AFFF), the drain time was enhanced to 240, 210, and 240 sec respectively. The DBSS(I-a) did not exhibit success in the sealability test individual without organic additives, but after formulating it as AFFF (with organic additives), a stable film of sealability test was obtained (2 minutes). The organic additives may be play an important role to decrease the foam bubble size of this anionic surfactants which let its foam bubbles to pass via the screen mesh to form a stable sealing film.

Table 12: Effect of pH on foam properties and sealability of DBMSA(I-b)

Foam Sample	pH	Sealability Test	Sealability Time /min	Expansion Ratio (ER)	25% Drainage Time/sec
1%	2	SF	4	2.9	85
	4	SF	4	2.9	85
	8	SF	4	2.9	85
	10	SF	4	2.9	85
3%	2	SF	3.5	4.6	135
	4	SF	3.5	4.6	135
	8	SF	3.5	4.6	135
	10	SF	3.5	4.6	135
6%	2	SF	3	5.3	165
	4	SF	3	5.3	165
	8	SF	3	5.3	165
	10	SF	3	5.3	165

Table 13: Effect of electrolyte (NaCl) on foam properties and sealability of DBMSA(I-b)

Foam Sample	NaCl	Sealability Test	Sealability Time /min	Expansion Ratio (ER)	25% Drainage Time/sec
1%	1%	SF	3	2.1	60
	2%	RF	-	1.6	45
	3%	RF	-	1.1	30
3%	1%	SF	2.5	3.6	105
	2%	RF	-	2.7	90
	3%	RF	-	2	60
6%	1%	SF	2	4.3	120
	2%	RF	-	3.3	100
	3%	RF	-	2.3	75

Table 14: Foam properties and sealability for some selected foaming agents without organic additives

Foaming agent	Sealability Test with screen	Sealability Time /min	Sealability Test without screen	Sealability Time /min	Expansion Ratio (ER)	25% Drainage Time/sec
CU	SF	2	SF	20	5.9	240
DBMSA	SF	3	SF	17	5.3	165
DBTS	SF	2	SF	12	4.4	135
DBSS	RF	-	SF	10	5.6	180

CU is the current used (AFFF 6%) in Qarun Petroleum Company.

Table 15: Effect of organic additives on foam properties and sealability for some AFFF formulations*

Foaming agent	Sealability Test with screen	Sealability Time /min	Sealability Test without screen	Sealability Time /min	Expansion Ratio	Drainage Time/sec
CU	SF	2	SF	20	5.9	240
DBMSA	SF	4	SF	22	5.9	240
DBTS	SF	3	SF	20	5	210
DBSS	SF	2	SF	17	6.1	240

Formulation: is a mixture of aqueous film forming foam and organic additives (diethylene glycol monobutyl ether and sod. dioctyl sulfosuccinate).